

## **NOTE TO USERS**

**The original manuscript received by UMI contains pages with light and indistinct print. Pages were microfilmed as received.**

**This reproduction is the best copy available**



**Isolation of a potential gene for obesity  
in a transgenic mouse**

BY

PEIYI FAN

A Thesis  
Submitted to the Faculty of Graduate Studies  
in Partial Fulfillment of the Requirements  
for the Degree of

MASTER OF SCIENCE

Department of Medical Microbiology  
University of Manitoba  
Winnipeg, Manitoba  
© December, 1998



**National Library  
of Canada**

**Acquisitions and  
Bibliographic Services**

**395 Wellington Street  
Ottawa ON K1A 0N4  
Canada**

**Bibliothèque nationale  
du Canada**

**Acquisitions et  
services bibliographiques**

**395, rue Wellington  
Ottawa ON K1A 0N4  
Canada**

*Your file Votre référence*

*Our file Notre référence*

**The author has granted a non-exclusive licence allowing the National Library of Canada to reproduce, loan, distribute or sell copies of this thesis in microform, paper or electronic formats.**

**The author retains ownership of the copyright in this thesis. Neither the thesis nor substantial extracts from it may be printed or otherwise reproduced without the author's permission.**

**L'auteur a accordé une licence non exclusive permettant à la Bibliothèque nationale du Canada de reproduire, prêter, distribuer ou vendre des copies de cette thèse sous la forme de microfiche/film, de reproduction sur papier ou sur format électronique.**

**L'auteur conserve la propriété du droit d'auteur qui protège cette thèse. Ni la thèse ni des extraits substantiels de celle-ci ne doivent être imprimés ou autrement reproduits sans son autorisation.**

0-612-35058-4

**THE UNIVERSITY OF MANITOBA  
FACULTY OF GRADUATE STUDIES  
\*\*\*\*\*  
COPYRIGHT PERMISSION PAGE**

**ISOLATION OF A POTENTIAL GENE FOR OBESITY IN A TRANSGENIC MOUSE**

**BY**

**PEIYI FAN**

**A Thesis/Practicum submitted to the Faculty of Graduate Studies of The University  
of Manitoba in partial fulfillment of the requirements of the degree**

**of**

**MASTER OF SCIENCE**

**Peiyi Fan©1998**

**Permission has been granted to the Library of The University of Manitoba to lend or sell copies of this thesis/practicum, to the National Library of Canada to microfilm this thesis and to lend or sell copies of the film, and to Dissertations Abstracts International to publish an abstract of this thesis/practicum.**

**The author reserves other publication rights, and neither this thesis/practicum nor extensive extracts from it may be printed or otherwise reproduced without the author's written permission.**

**I dedicate this thesis to my dear parents**

## Abstract

The objective of this research was to identify the genomic segments flanking the transgene LTR-tat3 in obese mouse, based on the hypothesis that the obese phenotype is the result of the genomic alteration caused by the integration of a transgene LTR-tat3. Two PCR strategies were applied to amplify the mouse genomic sequences flanking the LTR-tat3 insert. The inverse PCR approach was tried but was not successful. This may be due to the inappropriate DNA fragment sizes produced by the restriction digestion or incomplete digestion. The arbitrary PCR approach was then utilized to amplify the flanking sequences. For the left junction of LTR-tat3 insert, a set of twenty 10-mer arbitrary primers (OPA) were each used separately in conjunction with a specific primer complementary to the LTR sequence. Of the 20 OPA primers, nine produced positive bands with Southern blot analysis. These nine positive bands are potentially target sequences flanking LTR-tat3 insert by virtue of the tandem array of multiple LTR-tat3 transgene. For the right junction of LTR-tat3 insert, a modified arbitrary PCR — TAIL-PCR method was applied using three nested specific primers with a set of arbitrary degenerate primers (AD) as well as interspersed asymmetric and symmetric PCR cycling to geometrically favor amplification of the desired target sequence over nonspecific products. Of the four AD primers, the AD1 primer produced a band of 1100 bp that hybridized with the LTR-tat3 specific DNA probe. These probe positive fragments can be used as templates for making new specific primers for further

**chromosomal walking to identify additional sequences adjacent to the transgene.**

## **Acknowledgements**

I would like to thank everyone who has given me help and encouragement in the process of my graduate training and completing my thesis.

First, I would like to thank Dr. Francis Jay for his supervision, direction, patience, and advice. He has taught me how to learn and to do experiments with scientific thinking.

I would also like to thank Dr. Robery Shiu and Dr. Michelle Alfa for their time, support, suggestions and evaluation of this work.

Special thanks are given to all those who have been supporting me and taught me molecular biology techniques and skills. Thanks to Caixia, Dongji, Yvong, Barb, Alison, Emma, Ling-ling, Christein, Luo for their consistent help and friendship.

Finally, a special thanks to Theresa, Sharon, Zeena for their kindness and help.

## Table of Contents

	<b>Page</b>
<b>Literature Review</b>	1
Genetic aspects of obesity	1
Strategy for obesity study	5
The five cloned mouse obese genes	11
1). <i>Agouti</i> gene	11
2). <i>Fat</i> gene	13
3). <i>Tub</i> gene	15
4). <i>ob</i> gene	16
5). <i>db</i> gene	18
<b>Introduction and Hypothesis of the project</b>	22
<b>Materials and Methods</b>	27
<b>I. Materials:</b>	27
i) Construction of the pHIV/LTR-tat3 vector	27
ii) Generation of transgenic mice	27
<b>II. Methods:</b>	28
A. Transformation of E.coli (LE392) with pHIV/LTR-tat3 by Electroporation	28
B. Large-scale preparation of plasmid pHIV/LTR-tat3	29
C. Purification of pHIV/LTR-tat3 by CsCl/Ethidium Bromide Equilibrium Centrifugation	30

D. Preparation of genomic DNA from mouse liver tissue	31
E. Restriction endonuclease digestion of DNA	32
F. Ligation of digested mouse DNA	34
G. Purification of ligated DNA by phenol extraction and ethanol Precipitation	34
H. Electrophoresis of DNA	35
I. Gel purification of DNA fragments with GeneClean II kit	35
J. Detection of the LTR-tat3 insert in the transgenic mouse genome	36
K. Amplification of the sequences adjacent to the transgene by inverse PCR	37
L. Amplification of the sequences adjacent to the transgene by Arbitrary PCR	39
M. Amplification of the sequences adjacent to the transgene by Thermal Asymmetric Interlaced PCR (TAIL-PCR)	41
N. Transfer of DNA to nitrocellulose membrane	44
O. Radioactive labeling of DNA	46
P. Hybridization of DNA	48
Q. Automatic DNA sequencing	49
<b>Results</b>	50
I. The detection of the LTR-tat3 insert in the H2 transgenic mouse chromosome	50
II. The size of the vector fragment integrated with LTR-tat3	50
III. Inverse PCR (IPCR)	53

IV. Arbitrary PCR (APCR)	57
V. TAIL-PCR	60
VI. Sequencing analysis of the “Southern blot positive” DNA fragment	70
<b>Discussion</b>	75
<b>References</b>	86
<b>Appendix I</b>	100

**List of Tables**

Table.1	Transgenic mouse models with altered body fat	9
Table.2	Obesity genes identified in rodents	10
Table.3	Varous conditions for arbitrary PCR	41
Table.4	Cycling conditions used for TAIL-PCR	44
Table.5	Primer design for all PCR reactions	39

**List of figures**

Fig. 1	Construction of the pHIV/LTR-tat3 plasmid	28
Fig. 2	Schematic diagram of inverse PCR (IPCR)	25
Fig. 3	LTR/tat3 integration in tandem array	80
Fig. 4	Determination of the length of flanking segments of LTR-tat3 insert in vector pML	55
Fig. 5	Schematic diagram of the two strategies for PCR-cloning of the flanking sequences at the LTR-tat3 integration site	26
Fig. 6	Schematic diagram of TAIL-PCR strategy	43
Fig. 7	PCR of LTR-tat3 insert in transgenic obese H2 mouse chromosome	52
Fig. 8	Southern blot of the PCR amplified LTR-tat3 insert	53
Fig. 9	Inverse PCR of LTR-tat3 transgenic H2 mouse DNA	56
Fig.10	Southern blot analysis of IPCR products	57
Fig.11	Arbitrary PCR of left junction of LTR-tat3 transgene	59
Fig.12	Arbitrary PCR of left junction of LTR-tat3 insert with Arbitrary primers (OPAs) and specific primer LTR/L-2	60

Fig.13 Arbitrary PCR of left junction of LTR-tat3 insert with arbitrary primers (OPAs) and specific primer LTR/L-2	62
Fig.14 Arbitrary PCR of left junction of LTR-tat3 insert with arbitrary primers (OPAs) and specific primer LTR/L-2	63
Fig.15 Arbitrary PCR of left junction of LTR-tat3 insert with arbitrary primers (OPAs) and specific primer LTR/L-2	64
Fig.16 Southern blot analysis of arbitrary PCR products	65
Fig.17 TAIL-PCR of right junction of LTR-tat3 transgene	68
Fig.18 Southern analysis of TAIL-PCR products	69
Fig.19 Re-PCR agarose gel analysis and Southern blot analysis of gel -purified positive APCR products with the same set of primers	66
Fig.20 Confirmation of TAIL-PCR product with AD1 by gel and Southern blot analysis	70
Fig.21 The sequence of the TAIL-PCR-amplified 1100 bp fragment with the specific primer SP3	72
Fig.22 The sequence of the TAIL-PCR-amplified 1100 bp fragment with the arbitrary degenerate primer AD1	74

## **Literature Review**

Obesity is the most common nutrition disorder of industrialized societies and the prevalence is increasing in many developing countries as well [1]. Obesity can be viewed as an indicator of diverse underlying metabolic and physiologic dysregulations rather than a disease entity per se. This complex disorder is caused by an imbalance between energy intake and energy expenditure. These two processes are coordinately regulated by vegetative centers in the central nervous system, so as to maintain a relatively constant level of energy storage [2,3]. This concept of bodyweight “set point” implies that a set point of energy storage is controlled by multiple genes through complex regulatory pathways which respond to variation or perturbation in energy balance. Mutations in these genes may disrupt normal metabolism or prevent orderly adaptive metabolic or physiologic change and can thus result in dysregulation leading to obesity. Most human obesity is of complex multifactorial phenotypes influenced by multiple affactors including social, behavioral, physiological, metabolic, cellular and molecular domains [4]. It is critical to understand the etiology of the disorder in terms of the fundamental underlying mechanisms. In the last few years, major progress has been made toward the identification of genetic and environmental etiological factors.

### **Genetic aspects of obesity**

In recent years, a handful of studies have highlighted the importance of genetic factors in the etiology of obesity. Based on several lines of evidence, it is clear that genetic factors play an extremely important role in the development of this debilitating condition, despite the strong evidence of the role of environmental factors.

Adoption studies have shown that there is a significantly stronger correlation between the bodyweights of adoptees and their biological parents in comparison to their adoptive parents' [5], which suggests that genetics were more important than environment regarding their eventual adult weight.

In a study of twins [6], a group of identical twins were tested to detect their response to overfeeding. It was found that although their body weight increased, the difference in increase was very much closer within twins than between twins, suggesting that the response to overfeeding had a strong genetic component. In addition, variation in basal metabolic rate among individuals has been shown to be partly due to genetic differences [7]. In this study, the genetic effect for resting metabolic rate (RMR) was studied in 31 pairs of parent-child, 21 pairs of dizygotic (DZ) twins, and 37 pairs of monozygotic (MZ) twins. The heritability of RMR reached about 40% of the variance remaining after adjustment for age, gender and fat free mass, suggesting that there is indeed an effect of the genotype on the RMR.

It is interesting that some particular populations (e.g. Pima Indians) are especially susceptible to become obese, also suggesting the genetic predisposition to obesity; as a population, their biological predisposition to obesity is well expressed in the shared environment.

Several genetic epidemiological studies of interaction between genes and the environment have shown that heritability levels of body mass index (BMI), which is used as a measure of obesity, vary according to the design of the study [9]. The heritability is highest with twin studies (50-80%), intermediate with nuclear family data (30-50%), lowest in adoption studies (10-30%). However, when several types of relatives are used jointly in the same design, the heritability estimates cluster around 25-40% of the age- and gender-adjusted phenotype variance. The common familial environmental effect is marginal. This demonstrates that there is a heritability factor in BMI and the heritability is different among different groups of people due to genetic variation to human obesity. It was estimated that the risk of obesity is about two to three times higher for an individual with a family history of obesity and it increases with the severity of obesity [10]. Therefore, genetic influences clearly have a major effect in determining BMI and its extreme variant—obesity, while environmental factors modify these genetic influences by either enhancing or limiting weight gain in susceptible individuals. These phenomena can be explained by the concept of “set point” in genetic transmission that suggests genetic factors are preeminent in determining the level at which energy stores are set in a particular individual [11].

The most exciting advances made in the field of obesity over the last few years is that several obesity-related single genes in animals have been cloned, providing a new basis for understanding the genetic mechanisms and molecular basis of obesity development [8].

Taken as a whole, it can be demonstrated in Bouchard's words [6] that "each of the main components of the energy balance relationship has a genetic basis. A certain genetic makeup can give an individual a predisposition to obesity, and the appropriate environment can lead to the phenotypic expression." The citation is a good explanation for the concept, proposed by Greenberg [12], that in an individual there is a set of "susceptibility genes" which increase susceptibility to obesity but are not necessary for the obese phenotypic expression. It merely lowers the threshold for an individual to develop obesity; whereas "necessary genes" are the direct cause of the phenotype when they are mutated. The cases of necessary loci resulting in obesity represent only a small fraction of the obese population [13].

These findings mentioned above have led to a search for the underlying causes of obesity in both animal models and human. A major new progress in the obesity research field is the identification of specific genes that may be involved in a genetic predisposition to obesity. The cloning of genes predisposing an individual to obesity will yield considerable insights into the molecular genetic mechanisms that control body composition through the balance between food intake and energy expenditure [14,15]. Some obese phenotypes are influenced by major gene effects, where single genes play a major role within certain families, particularly morbid obesity such as the prader-Willi, Bardet-Biedl, Alstrom, and Cohen syndromes, but the gene involved may vary from family to family[16-18]. Except for these single-gene-mutation-induced obese phenotypes, most human obesity is a phenotype expressed through polygenic inheritance with genetic heterogeneity as well as environmental influences on phenotypic expression,

which is a complex multifactorial system with networks of gene-gene and gene-environment interactions, and the additive effects of multiple genes with each having small effects on a phenotype can lead to the polygenic phenotype. However, the identification of major genes will add to the understanding of the genetic mechanism of the polygenic obesity. Genetic heterogeneity may become a major challenge in current genetic studies of the obese phenotype and requires large pedigree materials and statistical evaluations. Therefore, the use of animal models is essential to the understanding of the genetic basis of obesity and will unravel potential candidate obese genes for further studies in humans.

### **Strategy for obesity study**

An overview of approaches currently applied to identify obesity-related genes is outlined here. The search for the obesity-related genes requires multifaceted approaches, basically including the following strategies [90]:

- the study of candidate genes for obesity;
- a genome-wide search using quantitative trait locus (QTL) analysis with genetic marker library covering the human genome.
- The study of animal models and extrapolation to human homologous regions;
- The study of human obesity syndromes.

The candidate gene approach is based on the current knowledge of the physiopathology of obesity, especially the pathways related to the regulation of energy

balance or to adipose tissue biology. Genes encoding molecules such as receptors, hormones, transporters and other key elements of the pathways are thought to be candidate genes. Another resource for candidate genes is the comparative genetic maps between man and mouse [91]. Among the candidate genes only a few have clear evidence of linkage to human body fat such as TNF $\alpha$ , adenosine deaminase and melanocortin-3 receptor [21,22].

It is known that in human genome there are highly homologous genes with rodent genes [23,24]. Based on the knowledge of syntenic relationship between mouse and human, the cloned mouse obesity genes can be logically considered to be candidate genes for human obesity and therefore were studied on whether the rodent mutations were actually present in human and whether these genes play any role in the human obesity susceptibility. However, although human homologs of the murine obesity loci have been identified, they do not appear to be associated with human obesity [25]. No mutation in humans has been shown in linkage studies performed so far to be responsible for the susceptibility to obesity. It is probably because although the murine and human homologs may be almost structurally identical, their expression in mouse and human may be very different due to tissue specific differences in the regulation of their transcription. In addition, the mouse obesity phenotypes are observed on highly inbred genetic backgrounds, namely congenic. Under these conditions, a gene which clearly has a major impact on quantitative traits when observed on an inbred background may have a smaller impact when they occur on an outbred background (e.g. in the wild). Thus, although the genes involved in determining obesity phenotypes in the mouse are logical candidate

genes for the human obesity, each gene might not be the same genetic basis for the human obese phenotypes. However, the cloning of the murine obesity genes has opened a door to investigations and understanding of the genetic mechanism of the obesity disorder.

So far, several candidate genes were investigated for their potential effects on obesity [35]. They include the  $\beta_3$ -adrenergic receptor gene, the uncoupling protein gene, the insulin receptor substrate-1 gene, the glucocorticoid receptor gene, the leptin gene, the leptin receptor gene, the agouti signaling protein (ASP) gene, the tubby gene, the TNF $\alpha$  gene, the peroxisome proliferator activated receptor (PPAR) genes, CCAAT enhancer binding protein (C/EBP) genes and the high mobility group (HMG) DNA-binding protein genes.

The identification of multiple genes leading to a complex phenotype requires different strategies from classical single gene studies [69]. It relies mainly on the linkage and association studies with various kinds of genetic markers. The quantitative trait locus (QTL) linkage approach is a powerful method for studying the polygenic complex system both in animal and human. This method is based on the genetic segregation by crossing of informative inbred strains or by studying pedigree and then followed by scan of the genome with a set of genetic markers for the specific chromosomal region where the candidate genes responsible for the polygenic traits may reside. It yields an estimate of where on the genome the genes responsible for the phenotype are located. The strength of QTL analysis is in that it can identify non-Mendelian genes that interact with each other and with environmental factors to produce obese phenotype. It is also

possible to perform a random genome-wide search for candidate genes contributing to human obesity with the genetic marker libraries covering the entire human genome by studying large single-pedigree nuclear families, or affected pedigree member [25], however, most association and linkage studies performed so far have yielded negative results [20,26]. No mutation has been found to link to a common form of human obesity. As Bouchard, C. [92] put it “this is particularly striking when one realizes that there is not one obese human whose excess body mass and body fat can be explained by a specific mutation in one of the genes exerting its effects in relevant energy balance pathways.” However, twenty-four QTLs have been identified in association with crossbreeding strains of mice or rats with variable susceptibility to obesity [19,20].

The use of obese rodent models as a tool in the study of complex genetic traits such as human obesity can overcome the difficulties inherent in the molecular analysis. The analysis of heterogeneous and polygenic traits is greatly simplified by using animal models. To date, several single-gene locus or polygenic mouse models for obesity have been used to identify mutations. In addition, genetically engineered animals such as gene “knock out” mice or transgenic mice with increased or decreased body fat are more powerful tool and can be a source of new insights into obesity [70-77]. Table 1. lists several transgenic and knock-out mouse models that have been found to alter body fat [89]. The advantages of using mouse models as a tool for the study of obesity are: (1) availability of inbred and congenic strains, (2) a dense genetic map and physical mapping tools, (3) highly homologous chromosome regions between mouse and human, and (4) easy to manipulate. That is why genetic studies of obesity in animals are much faster and

**Table 2. Obesity genes identified in rodents**

Gene	Gene product	Rodent Chromosome	Inheritance	Human Homologous Region	Action
ob(mouse)	leptin	6 (mouse)	recessive	7q31.3	signal of energy stores
db*(mouse)	leptin receptor	4 (mouse)	recessive	1p32	reception of leptin signal
fa*(rat)	leptin receptor	5 (rat)	recessive	--	reception of leptin signal
fat (mouse)	carboxypeptidase E	8 (mouse)	recessive	4q32	prohormone processing
tub (mouse)	phosphodiesterase	7 (mouse)	recessive	11p15.1	role in hypothalamic cellular apoptosis
agouti (mouse)	agouti signaling protein	2 (mouse)	dominant	20q11.2-q12	blocking of melanocortin -4 receptor

\*db and fa are homologues

**Table 1. Transgenic mouse models with altered body fat**

---

**Models with increased body fat:**

1. Reduction in brain glucocorticoid receptor by antisense mRNA.
2. Overexpression of corticotropin-releasing hormone.
3. Knockout of uncoupling protein (UCP) in brown adipose tissue.
4. Knock-out of  $\beta$ -3 adrenergic receptor.
5. Overexpression of GLUT-4 in fat.

**Models with decreased body fat:**

1. Knockout of the glut-4 gene.
  2. Overexpression of lipoprotein lipase (LPL) in muscle and cardiac tissue.
  3. Overexpression of uncoupling protein (UCP) in white adipose tissue and brown adipose tissue.
  4. Overexpression of the phosphoenol pyruvate carboxykinase (PECPK) gene.
-

more successful than in humans. In many ways, however, animal and human research methods are interactive and complementary. To date, remarkable progress has been made in the identification and characterization of the five obese genes mutated in monogenic mouse models (Table 2). The five obese genes cloned from obese mouse models are *agouti*, *fat*, *tub*, *ob*, and *db* genes. The cloning method, the biological function and the potential pathogenetic mechanism of these five obesity genes are reviewed below:

### *Agouti gene*

The first murine obesity syndrome to be characterized at the genetic level was the obese yellow mouse [28]. The cloning of the *agouti* gene was achieved by probing a mouse cDNA or genomic library with a genomic DNA probe from the  $Id^{Hd}$  insertional mutant which is a radiation-induced inversion mutation. This mutation ( $Is1Gso$ ) contains DNA breakpoints in the limb deformity (*ld*) and *agouti* loci. [28]. The human homolog of *agouti* was cloned afterwards using the mouse cDNA and named the *agouti* signaling protein (ASP) [27], which is 85% identical to the mouse gene at the nucleotide level and 80% identical at the amino acid level.

The wild-type *agouti* gene is normally expressed by cells of the hair follicle, encoding a 131-amino-acid protein with a consensus signal peptide [28]. The *agouti* protein acts as a transiently secreted paracrine factor by antagonizing the interaction between  $\alpha$ -melanocyte-stimulating hormone ( $\alpha$ -MSH) and its receptor on the melanocyte [29]. This normal *agouti* expression in mice results in black hairs with a

subapical band of yellow. In humans, this gene showed a more general expression.

Some dominant mutations at the agouti locus cause the increase in yellow pigment in the mouse coat and are associated with pleiotropic effects such as obesity, diabetes and increased susceptibility to tumors [30]. Over 25 mutations have been found in the agouti gene. Five are dominant mutations that resulted from an insertion of an intracisternal A-particle (IAP) element ( $A^{vy}$ ,  $A^{bvy}$ ,  $A^{iy}$ ,  $A^{iapv}$  allele, or from a deletion of genomic DNA between an upstream gene Raly ( $A^y$  allele) and the agouti gene, which juxtaposes the promoter and noncoding first exon of Raly with the first noncoding exon of the agouti gene, thereby bringing the coding region of the agouti gene under the control of the heterologous promoter [30].

The  $A^y$  mutation, arising spontaneously from an allele at the agouti locus on the mouse chromosome 2 [28], results in unregulated expression of the agouti protein in all tissues including adipose tissue. This ectopic and ubiquitous overexpression of the agouti gene leads to the obese phenotype. Experiments with transgenic mice expressing the agouti cDNA under the control of the  $\beta$ -actin promoter confirmed that ubiquitous expression of the protein induces the obese phenotype [30,31]. The  $A^y$  phenotype is an autosomal dominant, adult-onset obesity with insulin resistance, diabetes, and yellow coat color that is due to widespread ectopic expression of the agouti protein [28].

It has been shown that the intracellular free calcium concentration ( $[Ca^{2+}]_i$ ) in  $A^{vy}$  mutant is increased in skeletal muscle, and the degree of increase is closely correlated with the degree of obesity. An increase in  $[Ca^{2+}]_i$  and a corresponding increase in adipocyte fatty acid synthase activity were also observed in the skeletal myocytes or

adipocytes incubated in the presence of recombinant agouti protein [32,33]. Since it is acknowledged that the intracellular  $\text{Ca}^{2+}$  plays a role in mediating insulin action and dysregulation of  $\text{Ca}^{2+}$  flux is observed in diabetic animals and humans, it is speculated that the agouti protein has the potential to alter the signaling pathways of hormones involved in the regulation of fat storage by increasing calcium concentration, which would result in insulin resistance and hyperinsulinemia as observed in several systems [93-99], although the relationship between  $[\text{Ca}^{2+}]$  and insulin signal transduction is poorly understood. The agouti protein is known to antagonize the binding of the  $\alpha$ -melanocyte stimulating hormone to its receptors, preventing the rises in cAMP normally induced by this hormone in melanocytes [29]. It is speculated that excessive secretion of the agouti protein by the adipocytes could also induce a decrease in cAMP levels, reducing basal lipolytic rate and favoring fat storage [100].

The exact mechanism such as ectopical expression of tissue site or the receptor mechanism by which the agouti gene induces obesity is unclear. However, because agouti is expressed in the hypothalamus in mutant animals, a center of energy regulation in animals, it is possible that it functions as a central mediator [101]. In humans, the expression of the agouti homologue ASP in all tissues raises the possibility of comparable causes of obesity in some families. Up to now, however, no mutation in ASP related to obesity has been found. Moreover, the ASP gene has been located to human 20q11.2, but no significant linkage or association has been shown between the ASP locus and obesity.

***Fat gene***

The fat mutation leads to an autosomal recessive obesity phenotype including a range of abnormalities, such as progressive adult onset obesity, hyperinsulinemia and infertility [34].

The fat gene was identified using positional candidate gene approach. A distinction has to be drawn between the two concepts “candidate gene” and “positional candidate gene”. The former is a gene that could play a role in determining the phenotype because of its potential involvement in the physiopathology of obesity, whereas the latter is a gene that is being targeted primarily because of its location in a chromosomal region showing evidence of a relation with obesity together with its potential functions [35]. The fat gene has the same cytological and physical location as the carboxypeptidase E (cpe) gene (within 0.08 cM of cpe gene on mouse chromosome 8.), which plays a role in the processing of the proinsulin hormone and was a reasonable candidate gene for the fat phenotype. A missense mutation, or a single base substitution (serine→proline), was identified in the cpe gene, which abolishes cpe enzyme activity in a variety of neuro-endocrine tissues, such as pancreas, pituitary of mutant fat mice [36].

The enzyme carboxypeptidase E, expressed in pancreatic islets, processes prohormone intermediates (including proinsulin) by removing the C-terminal arginine residues from insulin following C peptide cleavage; this mutation which abolishes enzyme activity [36] results in a proinsulin processing defect and a corresponding biologically less active circulating insulin. This is supported by the observation that the mutant mice were very sensitive to insulin in spite of high levels of circulating insulin.

Carboxypeptidase E is also expressed in pituitary glands other than pancreatic islets and is involved in the sorting and proteolytic processing of a variety of neuropeptides [37]. Thus, the function of any of the signaling molecules or receptors in the regulatory pathways could potentially be impaired due to the cpe deficiency, which triggers obesity in the animal. Therefore, the exact mechanism still needs to be elucidated by which the loss of cpe activity leads to obesity.

### ***Tub gene***

The most recent obesity gene to be identified is tub, which is associated with autosomal recessive late-onset obesity and is accompanied by retinal degeneration and neurosensory hearing loss.

The tub gene was identified through positional cloning and encodes a novel and highly conserved 505 amino acid protein [102,103]. Sequence analysis indicates that it is unlikely to be a secreted factor or transmembrane receptor, suggesting a cytosolic location. The basis of the tub mutation was found to be a G to T transversion in a donor splice site that eliminated splicing of the carboxy-terminal intron and resulted in the longer transcript without the last exon but including the last unspliced intron. The tub gene transcript is detected by Northern hybridization in retina, testis, brain, particularly the hypothalamus and hippocampus. Its expression in the hypothalamus suggests that obesity in these mice may also stem from malfunction of signaling pathways in the satiety center.

The tub protein shares 62% homology with a putative mouse testis-specific

phosphodiesterase. It has been found that mutations in cGMP phosphodiesterase cause retinal degeneration in mice through apoptosis of photoreceptor cells triggered by an abnormal accumulation of cGMP [38]. It is therefore speculated that the mutated tub gene leads to late-onset obesity through the activation of apoptosis and gradual loss of function of hypothalamic nuclei involved in satiety or energy regulation. A well-conserved human tub gene has been cloned [39], but it is not yet known whether there are any mutations in this gene in obese humans.

### *ob gene*

The understanding of the mechanisms involved in energy regulation has been considerably advanced by the positional cloning of the *ob* gene in *ob/ob* mice with a profound obese phenotype [40]; these mice are the most extensively studied obese animal models. Positional cloning is an approach of isolation of a gene based on its position on a chromosome rather than on the knowledge of its protein product. In positional cloning, the mutant phenotype is used in mapping the mutant locus in genetic crosses or in pedigrees segregating for the phenotype. Genetic markers closely linked to the mutation can be used as starting points for chromosome walking to identify the target gene. The *ob* gene in mice was positioned on chromosome 6 close to a restriction fragment length polymorphism (RFLP) marker, D6Rck13 and also linked to the *Pax4* gene [54,55]. The characterization of the *ob* gene has disclosed an important regulatory pathway in energy balance, based on the earlier lipostatic set point hypothesis. The *ob* gene is expressed exclusively in adipose tissue, encoding a novel 167-amino acid

secreted protein, named leptin [40] (Greek: leptios, thin).

Two different mouse mutations were found in *ob* gene. A nonsense mutation (C→T transversion) in the original C57BL/6J *ob/ob* strain resulted in the change of an arginine at position 105 to a stop codon and thus a premature truncated polypeptide; the nature of another mutation is not yet known, but the lack of detectable mRNA by Northern blot analysis or RT-PCR in adipose tissue from the co-isogenic obese strain SM/CKC-+<sup>Dac</sup> *ob*<sup>2J</sup>/*ob*<sup>2J</sup> might be due to an alteration in the promoter region. Mutations in *ob* mice lead to either the synthesis of a prematurely truncated protein or defective leptin production. It is thought that leptin controls the size of the white adipose tissue depots by signaling or acts as a satiety factor, and as such provides a molecular basis for the lipostatic theory of energy regulation [2,3].

It has been shown that administration of recombinant leptin to *ob/ob* mice leads to a reduction in body weight, body fat, food intake, serum glucose and insulin. Conversely, the metabolic rate, body temperature and overall activity of these animals is increased [41-43]. It is proposed that the expression of the *ob* gene by adipocyte is subjected to nutritional regulation through a feedback loop. Fasting induces a decrease in the level of *ob* mRNA, which can be reversed on refeeding, and the circulating level of leptin changes in parallel to the mRNA in adipose tissue. In addition, a number of factors can also regulate the *ob* gene expression. These include insulin [44], glucocorticoids[45], β-adrenergic agonists [46], and cytokines [47]. The effect of β-adrenergic agonist suggests that there is sympathetically mediated suppression of *ob* gene expression, since the sympathetic system is a key component of the proposed feedback loop to adipocytes.

Mouse and human leptin sequences are 84% identical at the amino acid level [40]. However, no mutation has been observed from sequencing the coding region of the *ob* gene in human obesity [48-50]. On the other hand, genotyping with microsatellite markers covering the *ob* locus has suggested linkage of this region with extreme human obesity [51,52]. The observation that high levels of circulating leptin and “leptin resistance” are found in the vast majority of obese humans [48,53] further stimulated the interest in the identification of the receptor for leptin and the analysis of leptin signal reception.

### *db gene*

The identification of the leptin receptor (OB-R) was realized with an expression cloning strategy which is an elegant functional cloning approach [56]. A cDNA expression library was constructed from the mouse choroid plexus and was transfected into COS cells and the cells were screened by probing with the tagged leptin (radiolabelled leptin and leptin-alkaline phosphatase fusion proteins). The cloning of the leptin receptor gene by virtue of leptin binding, followed by genetic mapping to position the gene within a narrow interval of the *db* locus on mouse chromosome 4 and sequencing of the gene to demonstrate that this gene was mutated in *db/db* mice [57,58] provided clear evidence that the *db* gene is the leptin receptor gene. The long-held view deduced from the elegant parabiosis experiments conducted by Coleman and colleagues over 40 years ago was eventually verified by the molecular cloning technology. In the parabiosis experiments, the circulatory systems of two animals, from different strains,

were connected to each other. It was shown that a circulating factor from a normal or from a db mouse could restore normal weight in an ob mouse, whereas this factor from a normal or from an ob mouse failed to cause this phenomenon in a db mouse [59]. The db mice exhibit a very similar obese phenotype to the ob mice. Human OB-R was found to share 78% sequence homology with that of the mouse. The fa gene, a mutation responsible for the obesity of the Zucker rat, also relates to the leptin receptor gene; this gene is a homolog to the db gene in mice [68]. OB-R is a single membrane-spanning receptor showing many features of the Class I cytokine receptor family that signals through the Jak/STAT pathway [56,60]. There are multiple forms of OB-R in both mice and humans. The extracellular domains of the long and short forms of OB-R are identical, whereas the intracellular domains are different in length and sequence composition, arising from alternative RNA splicing at the most C-terminal coding exon [57,58]. The short form OB-R mRNA is found in multiple mouse tissues, while the long form OB-R is expressed predominantly in the hypothalamus [60], especially in the regions (arcuate, ventromedial, paraventricular, and dorsomedial nuclei [61]) previously thought to be important in body weight regulation. The high levels of the short form in the choroid plexus may mediate uptake across the blood-cerebral spinal fluid barrier and couples ligand binding to the intracellular signaling action of leptin. Short OB-R forms may also play a role in clearance or as a source of soluble receptor. It is not clear why several distinct short OB-R forms exist. In db/db mice, this same alternative splicing event can still occur; however, a mutation present in the OB-R gene in db/db mice generates a new splice donor site, creating a new exon that is inappropriately inserted

into the transcript encoding the long intracellular domain and therefore resulting in a stop codon prematurely terminating the long intracellular domain. The db mutation is a single nucleotide substitution (G-T transversion) within an exon containing the extreme C terminus and 3'-untranslated region of the short intracellular domain form of OB-R. The truncated form OB-R due to db mutation in the hypothalamus may block the signal of satiety from leptin.

The genes immediately and directly regulated by the leptin/OB-R signaling pathway in the central nervous system have yet to be clearly characterized. Two groups have reported that leptin administration to ob/ob but not db/db mice significantly reduces arcuate neuropeptide Y (NPY) mRNA levels [65,66]. Since NPY is a potent central appetite stimulator and it also affects energy expenditure pathway for leptin function [62-64], an interaction between leptin and the NPY system could be possible [67]. The experiment with NPY knockout mice suggests that suppression of arcuate NPY can not be the sole mechanism for leptin regulation of body weight, and other central leptin targets may exist.

The study of leptin regulatory system is at its beginning, and the picture of leptin as one of a chain of regulators in the cascade effect is extending. No studies so far have identified defective ob and db genes as causal factors in human obesity. However, since ob and db gene products form a hormone-receptor regulatory system in energy balance, the identification of the ob and db gene has provided the first genetic framework on which a fuller understanding of the mechanism of metabolic regulation obesity can be built. This eventually may lead to the treatment and prevention of this widespread

disorder.

## **Introduction and Hypothesis of the project**

Human immunodeficiency virus (HIV) is a retrovirus in the lentivirus subfamily [78]. Tat is one of the two essential regulatory genes for regulating HIV gene expression and replication. The tat protein is a potent transactivator which up-regulates HIV-LTR-directed gene expression. It may also act as a growth factor to modulate the cellular gene expression [104,105]. It is well known that the retrovirus HIV causes various clinical manifestations associated with AIDS, including the acquisition of an immunodeficient state, the neurological disorders, and many types of malignancies [78,79]. In an attempt to identify the disease caused by the virus HIV genes, Dr. Gilbert Jay and colleagues produced transgenic mice expressing the tat gene by introducing the tat gene under the control of the HIV long terminal repeat (LTR) into the germline of mice [106]. As mentioned in the previous section, the introduction of exogenous genetic material into mice that have their genes responsible for energy regulation disrupted or knocked out as a result may lead to the bodyweight alteration of mice. Among the 6 founder mouse lines, one mouse line exhibited an obese phenotype, in addition to the dermal lesions resembling Kaposi's sarcoma (KS) shared by all the 6 founder lines. The effect of tat3 expression in skin was observed as a cancerous process of the dermal cells. At the early stage, hypercellularity of spindle shaped cells was observed in the dermis of 4-month old F1 male mice; at the advanced stage, hypercellularity of the dermis became marked and collagen had been replaced by spindle-shaped or fibroblastic cells; at the late stage, ~15% of the 12-18 month old male mice developed skin tumors similar to Kaposi's

sarcoma. The phenotype of dermal KS-like lesions can not be caused by the HIV-LTR itself or the integration site because the same phenotype occurs in all the founder mouse lines that apparently have different integration sites. On the other hand, the obese phenotype that occurs only in one transgenic mouse line cannot be explained by the inserted tat gene per se, because otherwise the other transgenic lines would also develop the same phenotype. Based on the facts we know, we hypothesize that the insertion of the exogenous DNA fragment has led to a disruption of an endogenous gene that encodes a protein directly or indirectly responsible for the obese phenotype. To test our hypothesis, the first and foremost important task was to clone the mouse genomic sequences flanking the LTR-tat3 from the insertion site in the obese transgenic mouse.

We made use of polymerase chain reaction (PCR) cloning technology to isolate the DNA fragment flanking the transgene. A number of PCR methods have been described for the purpose of isolating DNA from a sequence-unknown segment bordering a known sequence. Each of these methods has its advantages and disadvantages. For our experimental approach, we applied two different PCR technical strategies: inverse PCR (IPCR) [84] and arbitrary PCR (APCR) [107]. Both approaches were aimed at amplification of the adjacent mouse genomic sequences flanking the LTR-tat3 transgene. In IPCR, the transgenic mouse genomic DNA was first subjected to restriction digestion using an endonuclease that did not have a restriction site in the inserted sequence, which generated, among others, fragments that contain host sequence flanking the LTR-tat3 transgene. The fragments were then recircularized by ligation. The recircularized fragments containing the LTR-tat3 sequences were used as templates in

IPCR with two outward-reading primers complementary to the LTR-tat3 sequences, thereby amplifying the adjacent mouse DNA between the two inverse primers (Fig.2). The arbitrary PCR approach was applied differently in the upstream and downstream regions of the LTR-tat3 transgene. In an attempt to PCR amplify the left adjacent sequence flanking LTR-tat3 (Fig.5), one specific primer complementary to LTR sequence was used in conjunction with one out of 20 arbitrary primers. The right adjacent sequence was amplified by using 3 nested specific primers in a series of 3 successive PCR reactions, each one using one arbitrary degenerated primer and one of 3 specific primers complementary to the tat3 sequence. The method is called thermal asymmetric interlaced PCR (TAIL-PCR). The TAIL-PCR approach makes use of interspersing asymmetric and symmetric or high stringent and low stringent PCR cycling so as to geometrically favor the amplification of the target sequence initiating from the specific primers to the arbitrary degenerated primer, respectively. All the PCR products were screened by Southern blot hybridization with a DNA probe specific to the LTR-tat3 sequence. All successfully amplified target sequences should contain a segment of LTR or tat3 sequence and therefore should be detected by this screening method.

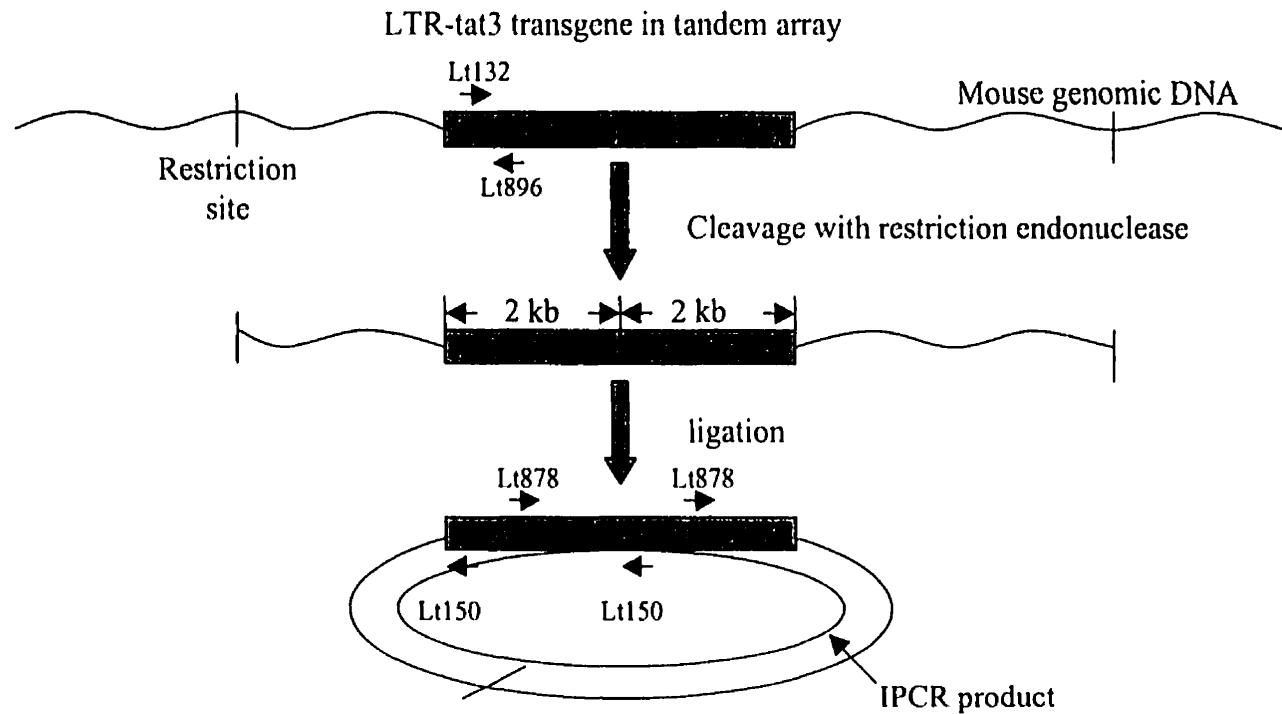


Fig.2: Schematic diagram of inverse PCR(IPCR)

The LTR-tat3 transgene is linked in tandem array at the integration site. The mouse genomic DNA was digested with *SacII*, *BclI*, *NcoI* none of which have restriction sites within the LTR-tat3 transgene. The fragments generated were recircularized by ligation, then used as IPCR template with two inverse primers ( Lt150, Lt878 ) based on the 3'-region in LTR-tat3 sequence. The two inward-reading primers (Lt132,Lt896) were used to detect the LTR-tat3 sequence. The number in the primer name denotes the start point of the primer in LTR-tat3 transgene with the first nucleotide of the LTR sequence as the beginning site. The <sup>32</sup>P-labeled probe was made by random priming with the whole pHIV/ LTR-tat3 plasmid as template.

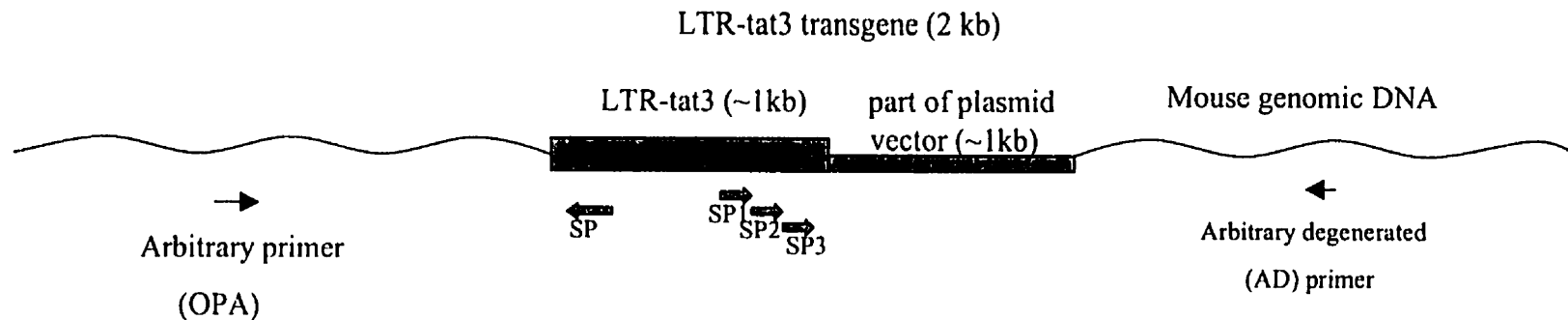


Fig.5: Schematic diagram of the two strategies for PCR-cloning of the flanking sequences in the LTR-tat3 integration site.

The left junction of LTR-tat3 was amplified with an arbitrary primer (OPA) and the specific primer (SP) using arbitrary PCR (APCR); the right junction of LTR-tat3 was amplified with an arbitrary degenerated (AD) primer and a set of 3 nested specific primers (SP1, SP2, SP3) complementary to the tat3 sequence using TAIL-PCR. The stippled bar represents LTR-tat3 transgene ( including LTR-tat3 and a part of plasmid integrated together ).The thin line represents the mouse genomic DNA.

## **Material and Method**

### **Materials**

#### **I. Construction of the pHIV/LTR-tat3**

To introduce the tat gene into mice, the pHIV/LTR-tat3 expression vector was constructed by placing the proviral 3' LTR and the authentic tat sequence from the AIDS-associated retrovirus strain 2 (ARV-2) into the pML cloning vector, which is a pBR<sub>322</sub> derived plasmid [80]. The complete LTR sequence contains the negative regulatory element and the positive regulatory element, with the transcriptional enhancer. The LTR also contains the tat-response element (TAR sequence) which is located within the R region. TAR acts as the target for tat transactivation. The tat sequence (101 amino acid) was derived by taking the 179-base pair (bp) XbaI-HindIII fragment, encoding amino acid residues 8-66, from ARV-2 and completing the missing 5' and 3' coding sequences with synthetic oligonucleotides (Fig.1). The entire unspliced sequence was put immediately downstream of the LTR sequence and upstream of the SV40 polyadenylation site. The recombinant expression vector was constructed in such a way that transcription is expected to start at the beginning of the R region, proceed across the tat coding sequence, and terminate within the SV40 poly (A) site. This pHIV/LTR-tat3 was provided by Dr. Gilbert Jay.

#### **II. Generation of LTR-tat3 transgenic mice**

A 2-kilobase (kb) KpnI-BglII fragment of the pHIV/LTR-tat3 containing the complete tat transcriptional unit was microinjected into fertilized eggs from

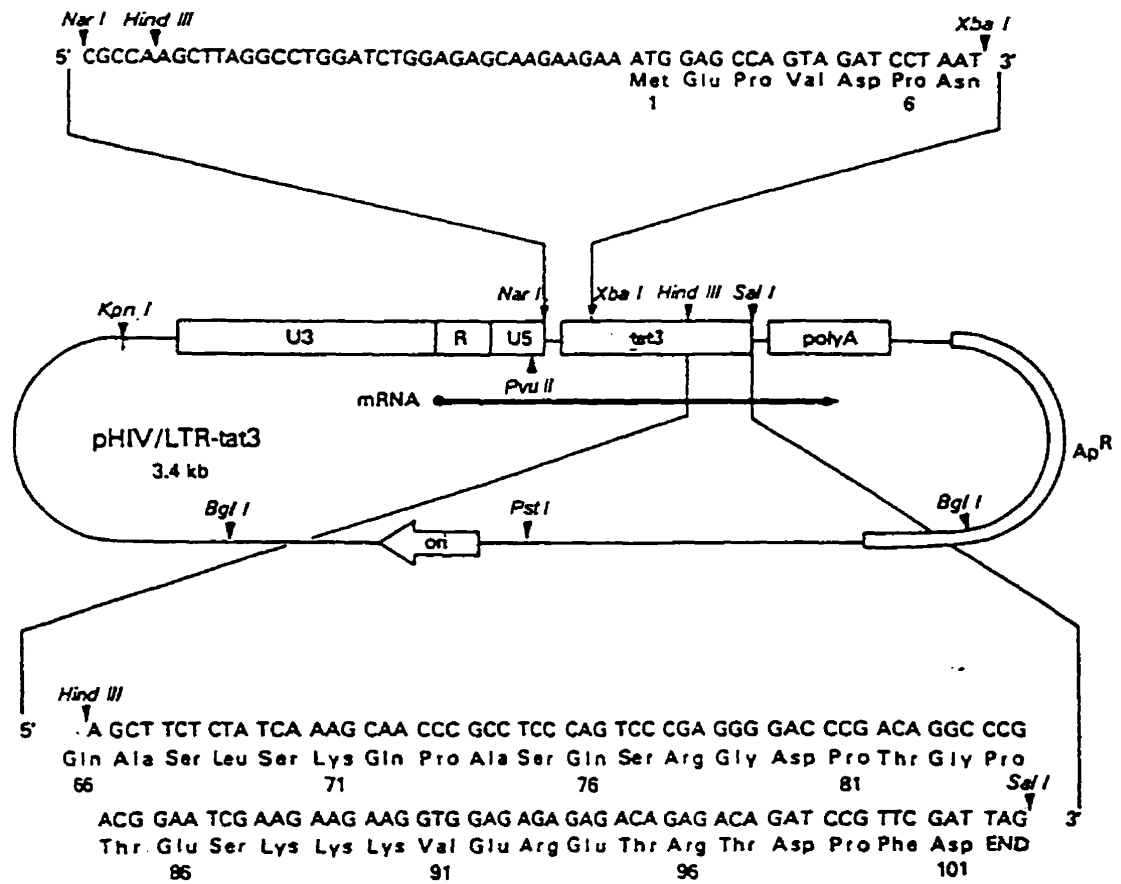


Fig. 1: Construction of the pHIV/LTR-tat3 plasmid.

The *tat3* was placed downstream of the HIV ARV-2 LTR, including the U3, R, and U5 regions, and upstream of a fragment containing the SV40 polyadenylation site and was inserted into the pML vector. The *tat* coding sequence was derived by taking an XbaI-HindIII fragment from the cloned HIV ARV-2 genome and completing the missing 5' and 3' sequences with the indicated synthetic oligonucleotides. The KpnI/BglII fragment containing LTR-*tat3* plus part of pML vector is then integrated into mouse genome, hence the name LTR-*tat3* transgene.

superovulated CD-1 female mice [Charles River Laboratories], which are outbred mice previously mated to (C57BL/6 X DBA/2) F<sub>1</sub> males [Jackson Laboratories]. Six founder-mice were identified by screening offspring for intact LTR-tat3 sequences by Southern blot hybridization, all of which showed a 2kb band presumably derived from a single integration site with multiple copies of the tat gene in a tandem array [106]. Founder H2 was the only mouse line expressing the obese phenotype. Back cross progenies were provided by Dr. Gilbert Jay.

## Methods

### **A. Transformation of Escherichia coli (E.coli) LE392 with pHIV/LTR-tat3 by Electroporation**

#### 1) Preparation of competent E.coli LE392 cell:

pHIV/LTR-tat3 in a 5 ml culture of Terrific Broth (TB, Appendix I, A) was inoculated from a single colony of E.coli LE392 agar plate and grown overnight at 37°C with shaking. One millilitre of the culture was used to inoculate 500 ml of TB that was grown with shaking to an OD<sub>600</sub>≈ 0.6. The culture flask was chilled on ice for 15-30 minutes. The culture was transferred to 4 sterile centrifuge tubes and centrifuged at 4000 x g for 15 minutes at 4°C. The supernatant was poured off, and the pellet was washed with ice-cold double distilled water (ddH<sub>2</sub>O) 200 ml/tube and centrifuged as above. The wash was repeated twice. The pellet was resuspended in 30 ml of 10 % (v/v) glycerol per tube, centrifuged at 2500 x g for 15 min, and then resuspended in 2 ml of 10 % (v/v) glycerol. The cells were frozen at -70°C in aliquots of 100 ul.

## 2). Electroporation of competent *E. coli* LE392

Electroporation was performed in a Gene Pulser™ device (Bio-Rad Richmond CA.). Forty microlitre of *E. coli* LE392 cell suspension and 1 ul of plasmid pHIV/LTR-tat3 (25ng) were mixed and transferred into a sterile, chilled 0.1 cm cuvette. The cells were pulsed in a chamber at 25 uF, with a resistance of 200  $\Omega$ ; the charging voltage was 1.8 kv and a pulse length of 4 sec. The cuvette was removed from the chamber and the cells were resuspended in 1 ml of SOC media (Appendix I, A). The cells were transferred to a sterile test tube and incubated at 37°C for 1 hour with shaking. Ten to twenty ul of cells were plated on a selective Luria-Bertani (LB)-agar plate containing 50 ug/ml ampicillin. The culture plate was incubated at 37°C overnight.

## B. Large-scale preparation of plasmid pHIV/LTR-tat3 from *E. coli* LE392

An alkaline lysis procedure was performed to isolate plasmid(s) propagated in *E. coli* LE392 cells. A 20 ml culture of LB media containing 50 ug/ml ampicillin was inoculated from a single colony (transformed by pHIV/LTR-tat3) and grown overnight at 37°C with shaking. Five millilitre of this culture was used to inoculate 500 ml LB-Amp that was grown at 37°C with shaking until OD600  $\approx$  0.6. Bacterial cells were collected by centrifugation in a JA-10 rotor at 6000 x g, for 10 minutes at 4°C. The cell pellet was resuspended in 4 ml of lysis buffer-Solution I (Appendix I, B) containing lysozyme (5mg/ml) and RNase A (50 ug/ml, added before use) and incubated at room temperature

for 10 minutes. The cells were lysed by the addition of 10 ml freshly prepared NaOH solution (Solution II, Appendix I, B), gently mixed, and placed on ice for 10 minutes. Finally, 7.5 ml of ice-cold Solution III (Appendix I, B) was added to the mixture to neutralize and precipitate the chromosomal DNA and proteins. After gentle mixing and incubation on ice for 10 minutes, insoluble material was removed by centrifugation at 20,000 x g for 10 minutes at 4°C. The supernatant was transferred to a separate tube and plasmid DNA was then precipitated by adding 0.6 volume of isopropanol followed by incubation at room temperature for 10 minutes. Plasmid DNA was collected by centrifugation at 15,000 x g for 10 minutes at room temperature. The pellet was washed with 2 ml 70 % ethanol. After centrifugation at 15,000 x g at room temperature for 15 minutes, the supernatant was discarded, and the pellet was air-dried and dissolved in 6 ml TE buffer for further purification by equilibrium centrifugation in cesium chloride (CsCl)-ethidium bromide gradient.

### **C. Purification of pHIV/LTR-tat3 by CsCl/Ethidium Bromide Equilibrium Centrifugation**

Cesium chloride (6.6 g ) was added to the tube containing pHIV/LTR-tat3 in 6 ml TE, mixed to dissolve, and 600 ul of ethidium bromide (EtBr, 10 mg/ml) was then added. After centrifugation at 2000 x g for 5 minutes at room temperature the red flocculent precipitate of ethidium bromide: protein complex was removed by pipette. The CsCl-DNA mixture was then heat sealed in a 5-ml ultracentrifuge tube (in 2 tubes) and

centrifuged at 350,000 x g for 20 hours at 20°C in a Beckman L8M ultracentrifuge (Beckman instruments Inc.). A needle was inserted into the top of the centrifuge tube to balance the air pressure and to control flow rate, the plasmid band was recovered to an Eppendorf tube by inserting a 20-G needle into the side of the tube 1 cm below the plasmid band with the beveled side up. The recovered plasmid band was extracted by adding an equal volume of TE saturated butanol to remove the EtBr. After vortexing and brief centrifugation, the organic layer was removed. This was repeated 3-4 times until both phases were clear and all the ethidium bromide was extracted from the aqueous phase. Two volumes of 100 % EtOH were added and the plasmid DNA was precipitated by incubating at -70°C for 1 hour. The DNA was recovered by centrifugation at 10,000 x g for 10 minutes at 4°C. The DNA pellet was resuspended in 200 ul of TE and quantified by UV spectrophotometry, then stored at -20°C until used.

#### **D. Preparation of genomic DNA from mouse liver tissue**

Frozen liver tissue from the H2 obese mouse was quickly ground into powder in liquid nitrogen. Four hundred milligrams of liver tissue powder were suspended in 4.8 ml digestion buffer (Appendix I, B) (1.2 ml/100mg tissue) containing proteinase K (0.1 mg/ml). The mixture was then incubated at 50°C for 18 hours with shaking. An equal volume of phenol/chloroform (1:1) was added to the mixture, mixed gently, briefly centrifuged, and then the organic phase was discarded. This step was repeated 2 more times. An equal volume of chloroform/isoamyl alcohol (20:1) was added, mixed, briefly

centrifuged, and then the aqueous phase was transferred to a new tube. This step was repeated once. The aqueous phase was transferred into dialysis bag (cut size-6000~8000 molecular weight) and dialyzed against 300 ml TE buffer (pH 8.0) for 5 hour at 4°C. The TE buffer was changed 3 times, with an incubation interval of 8 hour between the changes. Residual RNA was removed by adding 0.1 % SDS, and 1ug/ml RNase, incubating for 1 hour at 37°C, followed by phenol/chloroform and chloroform/isoamyl alcohol extractions and dialysis, as described above. The DNA was quantified by UV spectrophotometry. Conversion unit is 1 OD = 50 ug/ml. The genomic DNA from wild type mice were obtained from Dr. Robert Shiu's Lab.

#### **E. Restriction endonuclease digestion of DNA**

##### **i.) Digestion mouse genomic DNA**

Mouse genomic DNA (1.4ug) was placed in a sterile Eppendorf tube. The digestion was set up as follows: 1.4 ug mouse genomic DNA, 1 x reaction buffer (according to the enzyme manufacturer's guideline), and 5 units of each of the following restriction endonucleases: Nco I, Sac II and Bcl I used in separate reactions. The volume of the reaction mixture was 20 ul. The components were mixed by a brief centrifugation then incubated at the temperature recommended by the manufacturer overnight to achieve complete digestion. As a positive control for the subsequent ligation of the genomic digests, pHIV/LTR-tat3 was digested with PstI which has a single cut in the vector sequence (Fig. 1). The samples were stored at -20°C until used.

ii.) Preparation of the LTR-tat3 Kpn I/Bgl I fragment for the DNA probe.

The reaction mixture contained pHIV/LTR-tat3 plasmid DNA (1.4ug), 1 x reaction buffer, and 20 units of Kpn I in a volume of 20 ul. The mixture was incubated at 37°C overnight. The tube was spun down to collect the contents, then 30 units Bgl I and an appropriate amount of reaction buffer and ddH<sub>2</sub>O were added to the reaction mixture to make up to 30 ul in volume. Again, the digest mixture was incubated at 37°C overnight. The Kpn I/Bgl I fragment of LTR-tat3 was then gel purified using the GeneClean II kit according to the manufacturer's instructions (BIO/CAN Scientific, Mississauga, ON).

iii.) Determination of the length of the vector sequence integrated with LTR-tat3

Because IPCR and APCR specific primers were designed based on the LTR-tat3 sequence to amplify the mouse genome DNA adjacent to the vector segment flanking LTR-tat3 sequence, it is necessary to determine the size of the vector segment integrated with the LTR-tat3 sequence. To determine the length of the vector segment, the plasmid pHIV/LTR-tat3 was separately digested with KpnI, BglI and double digested with KpnI/PvuII or BglI/PvuII. The digestion condition consisted of pHIV/LTR-tat3 200 ng, an appropriate amount of reaction buffer according to the enzyme manufacturer's guidelines, and 1 unit of the endonuclease. The reaction mixture was incubated at 37°C, overnight. The DNA digests were resolved in 1% (w/v) agarose gel and the size of the digested DNA fragments were determined using a molecular marker (100 bp DNA ladder) running in parallel to the DNA fragment.

## **F. Ligation of digested mouse DNA**

Circularization of a DNA molecule is optimally achieved using a diluted DNA concentration ( $\leq 3$  ug/ml) as this favors self-ligation of the DNA molecule. The ligation mixture was set up as follows: 1 x ligation buffer, 0.5 mM ATP, 1.2 ug restriction digested mouse DNA, and 1.2 weiss units T4 ligase (GIBCO BRL/Life technologies) in a 450 ul of reaction system. The reaction mixture was incubated at 12°C overnight.

The positive control was set up by mixing linearized (with PvuII) pHIV/LTR-tat3 (~2pg) with 1.2ug of wild-type mouse DNA digested with Sac II, Nco I, or Bcl I.

## **G. Purification of ligated DNA by phenol extraction and ethanol precipitation**

The ligation mixture described in section F was brought up to 100 ul. An equal volume of phenol/chloroform (1:1) was added to the DNA solution, the mixture was vortexed thoroughly and then microcentrifuged for 30 sec, at 11,000 x g. The aqueous phase was transferred to a new tube, and extracted with phenol/chloroform one more time. An equal volume of chloroform/isoamyl alcohol (20:1) was added, mixed, and then centrifuged at 11,000 x g. The aqueous phase was transferred to a new tube and this extraction was repeated once. A 1/10 volume of 3M sodium acetate, pH5.2 was added to the DNA solution and mixed. Two volumes of ice-cold 100 % EtOH was then added, mixed by vortexing and DNA was precipitated by incubating at -70°C for 1 hour

followed by microcentrifugation for 30 minutes at 11,000 x g. The DNA pellet was washed with 70 % EtOH, then air-dried and then dissolved in 5 ul ddH<sub>2</sub>O.

## **H. Electrophoresis of DNA**

The DNA fragments were separated by agarose gel electrophoresis in a H5 model horizontal electrophoresis unit (Bethesda Research Laboratories.) coupled to a Model 494 power supply (Instrumentation Specialties Company, Winnipeg, MB.). A 1 % w/v agarose gel was prepared by mixing 90 ml 0.5 x TBE buffer, and 0.9 g ultraPURE agarose (GIBCO BRL/Life Technology Inc., Gaithersburgh, MD) and then by heating to completely dissolve. Ethidium bromide (0.5 ml of a 10 mg/ml stock solution) was added when the gel solution cooled down to 40-50°C. The slots in the gel were formed with a comb. The DNA marker was warmed up at 65°C for 5 minutes before loading. An aliquot of the DNA samples or marker was mixed with 6 x loading buffer and loaded into a slot. Electrophoresis was performed at 75 volts for 3-4 hours at room temperature. At the end of the electrophoresis, migration of the first tracking dye was typically 3.5-4 cm from the bottom edge. The DNA bands were visualized using an UV transilluminator (Model TM-15, UVP Inc., Pittsburgh, PA). Gels were photographed with a Polaroid MP4 camera with a red filter using Polaroid Type 57 film.

## **I. Gel purification of DNA fragments with GeneClean II kit**

Kpn I/Bgl I digested fragments of pHIV/LTR-tat3 or PCR product band were excised from the agarose gel, and then purified following the protocol from the GeneClean II kit [BIO/CAN Scientific., Mississauga, ON]. Briefly, the gel slice was weighed and minced (1 mg equals approximately 1 ul). TBE modifier (0.5 volume) and NaI (4.5 volume) were added to a given volume of agarose. The tube containing the mixture was incubated at 54°C for 5 minutes, and the tube was shaken occasionally, until the gel completely dissolved. Five microlitres of GlassMILK suspension (silica matrix) was added to the solution, mixed and placed on ice for 30 minutes to allow maximum binding of the DNA to the silica matrix. The tube was shaken occasionally. The tube was then spun for 5 seconds at 11,000 x g to pellet the silica matrix with the bound DNA. The supernatant was completely removed. The pellet was resuspended in 400 ul of New Wash (GeneClean II kit) by pipetting back and forth. After a 5 sec spin, at 11,000 x g, the supernatant was discarded. This was repeated 2 more times. After the last bit of liquid was removed with a fine tipped pipette. The pellet was resuspended in a mixture of ddH<sub>2</sub>O and GlassMILK and then incubated at 54°C for 15 minutes. After a 30 second spin at 11,000 x g in a microfuge, the supernatant was carefully transferred into a new tube. The DNA elution procedure was repeated one more time, and then the DNA stored at -20°C until used.

**J. Detection of the LTR-tat3 insert in the transgenic mouse genome by Polymerase Chain Reaction (PCR)**

The LTR-tat3 insert in H2 mouse chromosome was amplified by PCR. Polymerase chain reaction contained: 1 x PCR buffer (Pharmacia, Baie d'Urfe', Quebec. see Appendix), 0.2 mM each dNTPs, 1 uM both upper and lower inward primers (based on LTR and tat3 sequences, Table 5), 2 units of Taq DNA polymerase (Pharmacia, Baie d'Urfe', Quebec.), and 1.4 ug mouse DNA in a volume of 25 ul. The thermal cycling condition was: 95°C for 5 min, 40 cycles of 95°C for 1 min, 58°C for 1 min, and 72°C for 3 min in the Gene ATAQ controller (Pharmacia LKB Biotechnology, Uppsala, Sweden).

#### **K. Amplification of sequences adjacent to the LTR-tat3 transgene by Inverse PCR (IPCR)**

The IPCR method [84] was modified as follows: the genomic DNA from obese transgenic mouse H2 was digested with a restriction endonuclease which has no cleavage site within the LTR-tat3 transgene sequence to produce sticky ends in the DNA fragment. The DNA fragments were then ligated using conditions favoring circularization, and used as template in a PCR without cleaving the DNA circles. Similar amplification efficiency was achieved with or without cleavage of the circular DNA template. The primers (Lt150, Lt878, Table 5) for IPCR, complimentary to nucleotide 150-132 and 878-896 sequences, were designed to amplify outwards into the adjacent mouse sequence (Fig.2.)

IPCR was carried out under the following conditions: 1x PCR buffer (Pharmacia, Baie d'Urfe', Quebec. see Appendix), 0.2 mM each dNTPs, 1uM both inverse primers, and

**Table 5. Primer Design for All PCR reactions**

Name	Sequence	Location in pHIV/LTR-tat3	Tm (°C)	Use
Lt132	5'-GGCTACTTCCCTGATTGGC	132 nt- 150 nt	58	For PCR of LTR-tat3
Lt896	5'-CGCTTCTTCCTGCCATAGG	896 nt- 878 nt	60	
Lt150	5'-GCCAATCAGGGAAGTAGCC	150 nt- 132 nt	60	For IPCR
Lt878	5'-CCTATGGCAGGAAGAAGCG	878nt- 896 nt	60	
LTR/L-2	5'-GCCAATCAGGG	150 nt- 140 nt	36	with OPAs for APCR
SP1	5'-GTGTTGCTTTCATTGCTACGCG	828 nt- 849 nt	60	For TAIL-PCR
SP2	5'-GCCAATCAGGGAAGTAGCC	878 nt- 896 nt	60	
SP3	5'-GGAGACAGCGACGAAGAGC	896 nt- 914 nt	61	
AD1*	5'-TGWGNAGWANCASAGA	N/A	47	
AD2*	5'-AGWGNAGWANCAWAGG	N/A	41	
AD3*	5'-CAWCGICNGAIASGAA	N/A	41	
AD4*	5'-TCSTICGNACITWGGA	N/A	41	

\*Key to Symbols: S=G or C, W=A or T, I=Inosine, N=A or C or G or T

1 unit of Taq Polymerase, and 1.4 ug of purified circularized mouse DNA in a volume of 25 ul. The thermal cycling profile was 95°C for 10 min, then 50 cycles of 95°C for 1 min, 55°C for 1 min, and 72°C for 3 min.

**L. Amplification of the left junction of the LTR-tat3 transgene by Arbitrary PCR (APCR)**

The arbitrary PCR approach relies upon specific priming on one end within the known sequence together with arbitrary priming on the other end with an arbitrary primer within the unknown flanking sequence [107]. The mouse genomic DNA at the left junction of LTR-tat3 transgene is enriched by repeated cycles of primer extension that favors the specific primer within the transgene, thus extending it into the flanking chromosomal DNA. This is followed by reduced hybridization stringency to allow the amplification of the enriched DNA fragment using a set of arbitrary primers (OPAs), each separately, and the same LTR-tat3 specific primer. The mouse chromosomal LTR-tat3 junction fragments are identified by Southern blot hybridization using a probe made based on pHIV/LTR-tat3 Kpn I/Bgl I fragment.

To maximize the quantity and quality of the PCR products, a PCR optimizer kit (Invitrogen Corporation, Carlsbad, CA) was used to provide a set of variant reaction conditions, mainly by varying the pH and  $Mg^{2+}$  concentrations as summarized in Table 3. A set of twenty 10-mer arbitrary primers (Operon Technologies, Alameda, CA) were utilized separately with a specific primer LTR/L-2 (11-mers, Table 5) in all the reactions. The reaction mixture contains 1 x PCR buffer (Pharmacia, Baie d'Urfe', Quebec,

**Table 3.** Various Conditions for Arbitrary PCR

---

pH	[MgCl <sub>2</sub> ]	
	2.0	2.5
8.5	A	B
9.0	C	D
9.5	E	F

---

A-F, the combination of pH and MgCl<sub>2</sub> concentration, were used to provide a variety of conditions for the arbitrary PCR to determine the optimal conditions.

Appendix), 2 mM or 2.5 mM MgCl<sub>2</sub>, 0.2 mM each dNTPs, 0.5 uM specific primer (LTR/L-2), 0.5 uM arbitrary primer OPA, 100 ng mouse genomic DNA, and 0.75 units of Taq polymerase (Pharmacia, Baie d'Urfe', Quebec). The reaction was carried out in a volume of 12.5 ul. The thermal cycling started with denaturation at 94°C for 5 min, then 5 cycles of primer extension that favors the specific primer LTR/L-2 at 94°C for 30 sec, 40°C for 1 min with a ramping speed at 4 sec/°C, and 72°C for 2 min, followed by PCR amplification with the LTR/L-2 and an arbitrary primer at 94°C for 30 sec, 36°C for 1 min with a ramping speed at 4 sec/°C and 72°C for 2 min for 40 cycles.

#### **M. Amplification of the right junction of the LTR-tat3 transgene by Thermal Asymmetric Interlaced PCR (TAIL-PCR)**

TAIL-PCR [85] is a variant arbitrary PCR and it was applied to the right junction of LTR-tat3 transgene. TAIL-PCR (Fig. 6) starts with a high stringency cycling (high annealing temperature) with the first specific primer (SP1, Table 5) complementary to the tat3 gene sequence and an arbitrary degenerate (AD) primer so that only the specific primer can efficiently anneal to the DNA template for extension by the polymerase. This is followed by one low-stringency cycle to allow some mismatch in the initial annealing of the AD primer, hopefully, within the tat3-flanking sequence to create annealing site(s) adapted for the AD primer in the next rounds of PCR. Then a reduced-stringency cycling is carried out (tat3- flanking ) as a compromise to make both primers anneal to the DNA template. The adjacent sequence is then preferentially

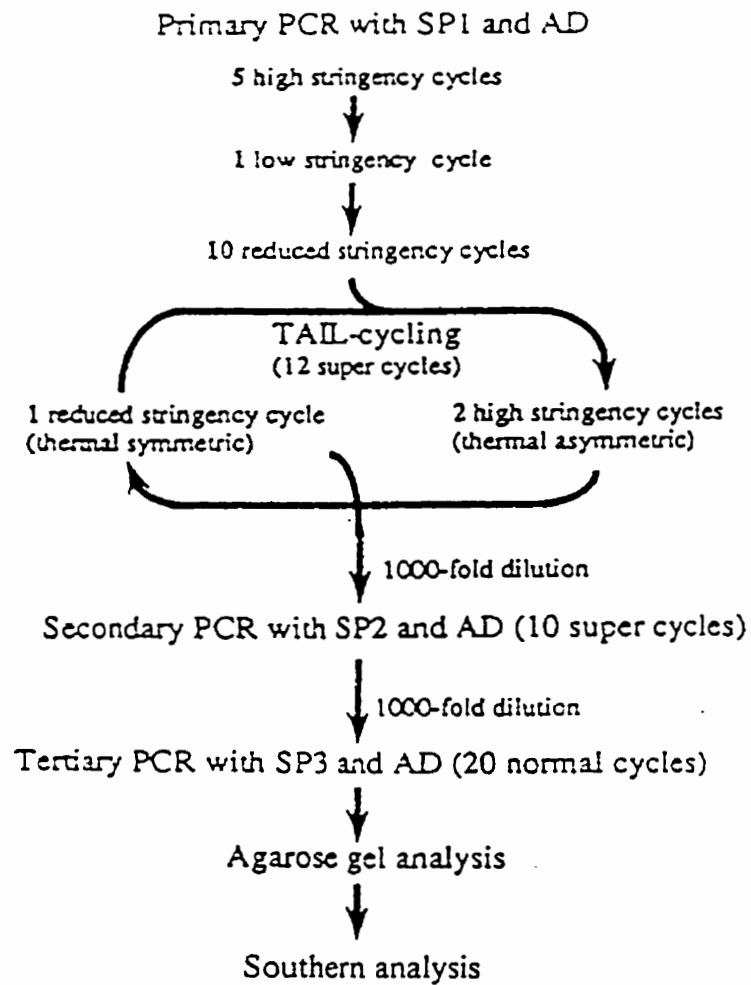


Fig.6: Schematic diagram of TAIL-PCR strategy.

TAIL-PCR includes primary, secondary and tertiary PCR using nested specific primers (SP1, SP2 and SP3) and arbitrary degenerate primer (AD).

Table 4. Cycling Conditions Used for TAIL-PCR

Reaction	Cycle No.	Thermal condition	
Primary	1	94°C (5min)	
	5	94°C (30sec), 52°C (1min), 72°C (2min)	
	1	94°C (30sec), 30°C (3min) 72°C (2min) ramp 4 sec/°C,	
	10	94°C (30sec), 44°C (1min), 72°C (2min)	
	20 <sup>a</sup>	94°C (30sec), 52°C (1min), 72°C (2min)	
		94°C (30dec), 52°C (1min), 72°C (2min)	
		94°C (30sec), 44°C (1min), 72°C (2min)	
		1	72°C (5min)
	Secondary	30 <sup>a</sup>	94°C (30sec), 56°C (1min), 72°C (2min)
			94°C (30sec), 56°C (1min), 72°C (2min)
		94°C (30sec), 44°C (1min), 72°C (2min)	
Tertiary	1	72°C (5min)	
	40	94°C (30sec), 44°C (1min), 72°C (2min)	
	1	72°C (5min)	

and geometrically amplified over all types of nonspecific products. TAIL-PCR includes 3 rounds of PCR cycling with 3 nested specific primers and each of the 4 arbitrary degenerate (AD) primers and was carried out as follows (The thermal cycling profiles are summarized in table 4) :

1. Primary PCR: the reaction conditions are 1 x PCR reaction buffer, 0.2 mM of each dNTP, 0.25 mM first specific primer (SP1), an AD primer (2.5uM for AD1, AD2 or 1.25 uM for AD3, AD4), 0.8 units of Taq polymerase, and 100 ng of mouse genomic DNA. The reaction mixture was in a total volume of 12.5 ul.

2. Secondary PCR: for secondary reactions, 1 ul aliquots of the primary PCR products were transferred to Eppendorf tube containing 99 ul ddH<sub>2</sub>O and mixed. Dilution aliquots (2.5 ul) were added to 22.5 ul of secondary PCR mixtures containing 1.1 x PCR buffer, 100 uM of each dNTP, 0.25 uM internal specific primer (SP2), the same AD primer used in the primary reaction (1.5 uM for AD1, AD2 or 0.75 uM for AD3, AD4), and 0.8 units of Taq polymerase.

3. Tertiary PCR: 1 ul aliquots of the secondary PCR products were diluted in 100 ul ddH<sub>2</sub>O, and 5 ul of dilutions were added to 45 ul tertiary PCR mixtures containing 1.1 x PCR buffer, 100 uM of each dNTP, 0.25 uM of the innermost specific primer (SP3), AD primer as in the preceding reaction, and 2 units of Taq Polymerase.

#### **N. Transfer of DNA to Nitrocellulose membrane**

After DNA fragments had been separated by electrophoresis, they were transferred to nitrocellulose by the method of Southern [108]. The gel was submerged in 500ml of denaturation solution and gently agitated for 45 minutes, with changing solution once during this period. This solution was removed and the gel was rinsed with distilled deionized water and submerged in 500 ml of neutralizing solution with gentle shaking for another 45 minutes, with changing of the solution once. The gel was then placed with the well-side down upon a Whatman 3MM filter paper wick saturated with 10 x SSPE (Appendix I, B). The filter wick extended over a glass plate support into a reservoir of 800 ml of 10 x SSPE. A nitrocellulose membrane (Micron Separations Inc.) having the same size as the gel was wet with 2 x SSPE and placed over the gel. Air bubbles trapped between the gel and the membrane were removed by gently rolling a glass pipette over the nitrocellulose. The nitrocellulose was overlaid with 2 pieces of 3MM Whatman filter paper saturated with 2 x SSPE and trapped air bubbles were removed as previously described. A stack of paper towels (15-20cm thick) was placed over the filters and held in place with a plastic plate in a horizontal level and a 500 g weight. DNA was allowed to transfer to the membrane overnight. After transfer was complete, the towelling and the filter papers were discarded, and the filter wick-gel-membrane "sandwich" was inverted on a plastic plate. The filter wick was carefully removed and the gel wells were marked on the membrane with an ink pen. The gel was removed. The nitrocellulose membrane was placed in 6 x SSPE for 5 minutes, then sandwiched between sheets of filter paper and baked for 2 hours at 80°C. After baking the membrane was stored at 4°C wrapped in Saran Wrap until used for hybridization.

## O. Radioactive Labeling of DNA

The DNA template was radioactively labeled by the random priming method using the Rad Prime kit [GIBCO/BRL Life Technologies.]. Fifty nanograms of DNA template (pHIV/LTR-tat3 KpnI/BglII fragment) in 20  $\mu$ l ddH<sub>2</sub>O was boiled for 5 minutes to be denatured. The tube was placed on ice at once. The reaction mixtures were added as follows: 1  $\mu$ l of 500  $\mu$ M dATP, dGTP, and dTTP, 20  $\mu$ l 2.5 x Prime buffer, 5  $\mu$ l  $\alpha$ -<sup>32</sup>P dCTP (10 uCi/ $\mu$ l) [New England Neuclei] and 1.5  $\mu$ l (1.5 units) of Klenow Fragment. The reaction mixture was mixed gently by tapping the tube followed by a brief centrifugation to bring down recalcitrant droplets. The reaction mixture was then incubated at 37°C for 20 minutes. The reaction was terminated by the addition of 5  $\mu$ l of stop buffer.

Incorporation of radiolabel and specific activity of the probe was evaluated by comparison of total and acid-precipitable (i.e. DNA-associated) radioactivity. Two pieces of Whatman 3M filter paper were each inoculated with 5  $\mu$ l of a 1:250 dilution in TE buffer of stopped reaction mixture, and was allowed to dry for 30 seconds. One of the filters was submerged into 10 % trichloroacetic acid (TCA) on ice for 15 minutes. The 10 % TCA was discarded. This was repeated 2 more times. Then the filter was washed with 95 % ethanol on ice for 15 minutes, with occasional shaking. The ethanol was discarded, and the filter was air-dried. This filter represented incorporated radioactivity while the other untreated filter represented total radioactivity. The two

filters were placed in separated scintillation vials and counted for radioactivity in  $\beta$ -liquid scintillation counter (Beckman, LS 5000CE).

Incorporation of label was calculated by the following formula:

$$\% \text{ incorporation} = \frac{\text{Acid-precipitable cpm}}{\text{total cpm}} \times 100$$

Specific activity (cpm/ $\mu$ g) of the probe, taking into account the dilution of the reaction mixture, was calculated as follows:

$$\text{Cpm}/\mu\text{g} = \frac{\text{Acid-precipitable cpm}/\mu\text{l}}{\text{ng DNA}/\mu\text{l}} \times 100$$

Specific activities varied from  $1 \times 10^8$ — $1 \times 10^9$  cpm/ $\mu$ g of DNA.

Separation of unincorporated nucleotide from labeled DNA was achieved by Sephadex G-50 chromatography. The reaction mixture was layered on a 4 ml Sephadex G-50 medium column and DNA was eluted with TE buffer. About 1.5 ml fractions were collected in sterile 1.5 ml Eppendorf tubes which were monitored for radioactivity by use of a Model 3 geiger counter (Measurements Inc., sweetwater, Texas). The fraction with the highest radioactivity (first peak) was evaluated for total and acid-precipitable counts. The DNA was denatured by boiling for 10 minutes followed by rapid cooling on ice until

just prior to being added to the hybridization solution.

#### **P. Hybridization of DNA**

The nitrocellulose membrane was wet with 6 x SSPE solution, then placed into a hybridization bottle with no bubbles between the membranes and the wall of the bottle. Ten ml of prewarmed prehybridization solution (Appendix I, B) was added to the bottle. The membrane was incubated in the gently rotated bottle at 42°C in an incubator (Robbins Scientific Corp., Sunnydale, CA.) for 2-4 hours. After prehybridization, the fluid was removed and 10 ml of warm hybridization solution containing the heat-denatured DNA probe was added. The membrane was then incubated overnight at 42°C as described above.

At the completion of incubation, the hybridization solution was drained into an aqueous radioactive waste container and the membrane was washed twice for 30 minutes in 200 ml of 2 x SSPE containing 0.1 % SDS followed by several washes with 200 ml of 0.2 x SSPE containing 0.1% SDS for 10 minutes. The number of washes determined by the residual reactivity detected by a geiger counter. All washes were performed at 65°C in a shaking waterbath. After the final wash the membrane was blotted dry between two sheets of filter paper and then wrapped in Saran wrap, and then was exposed to Kodak X-ray film (Interscience Inc., Markham, Ont.) in the presence of intensifying screens ( Dupont Cronex® Lighting-Plus YI, Markham, Ont. ) for varying lengths of time at - 70°C before development.

## **Q. Automatic DNA sequencing**

The “southern blot positive” fragments produced from the tertiary TAIL-PCR amplification were gel-purified using the Geneclean II kit (BIO/CAN Scientific, Mississauga, ON) and further purified by phenol:chloroform extraction. Briefly, an equal volume of water saturated phenol:chloroform:isoamyl alcohol (25:24:1) was added to the DNA sample, mixed by vortexing, spun and the top aqueous layer was transferred to a fresh eppendorf tube. An equal volume of chloroform:isoamyl alcohol (24:1) was added to the DNA solution to remove phenol, mixed, spun and the top aqueous layer was transferred to a fresh tube. The DNA was precipitated by adding 1/15<sup>th</sup> volume 3M sodium acetate pH 5.2, and 2.2 volumes 100% EtOH followed by incubation at -70°C for 30 min. The DNA was microcentrifuged at 11,000 x g for 30 min at 4°C. The liquid was removed and the DNA pellet was air dried for 10 min. Finally, the DNA pellet was dissolved in ddH<sub>2</sub>O, quantitated and sent for sequencing (ABI/PRISM, Cancer Foundation, Health Sciences Center, Winnipeg, MB.).

## Results

### **I. The detection of the LTR-tat3 insert in mouse chromosome:**

The insert LTR-tat3 in the mouse chromosome was first PCR amplified with two primers specific to the LTR-tat3 sequence and then subjected to Southern blot hybridization. Plasmid pHIV/LTR-tat3 was used as a positive control, undergoing PCR amplification with the same two specific primers. The <sup>32</sup>P-labeled probe was made specific to the LTR-tat3 insert. Fig.7 shows the PCR products from the transgenic mouse genomic DNA and plasmid pHIV/LTR-tat3. One of the multiple bands visible in the transgenic mouse DNA lane had the same size of ~750 bp as the only product band shown in the pHIV/LTR-tat3 lane which is expected to be the length between the two inward-reading primers (Lt132, Lt896) (Fig.2). The two 750 bp fragments both hybridized to the <sup>32</sup>P-labeled DNA probe in Southern blot analysis as shown in Fig.8. There was no PCR product from the wild-type mouse DNA (Fig.7) made by random priming with pHIV/LTR-tat3 plasmid as template. These results demonstrated that the transgenic mouse carries the LTR-tat3 sequence in its genome. There was no PCR product shown in lane D, which was the negative control of PCR reaction (Fig.7).

### **II. The size of the vector fragment integrated with LTR-tat3:**

A specific primer and a set of arbitrary primers were used for arbitrary PCR to amplify the mouse genomic sequences adjacent to the LTR-tat3 transgene. The specific primer was designed based on the LTR-tat3 sequence that is separated from the adjacent mouse genomic sequence by a part of the vector sequence that is integrated with LTR-

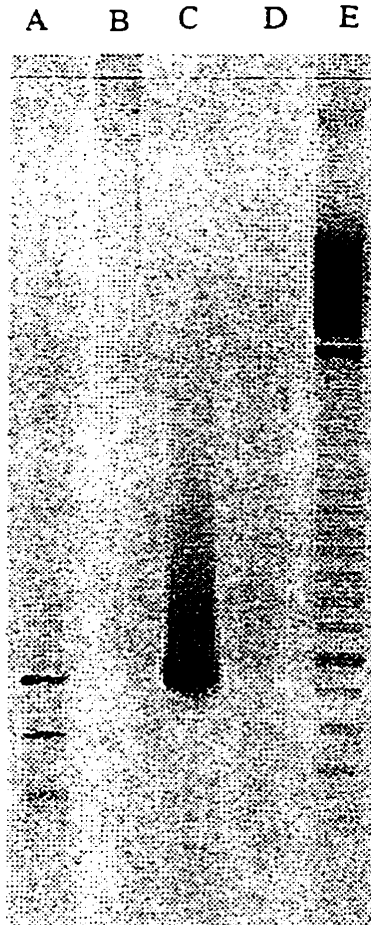


**Fig.7: PCR of LTR-tat3 insert in transgenic obese H2 mouse chromosome.**

The PCR reaction was performed with LTR-tat3 specific primers (Lt132, Lt896). Lane A contains PCR products amplified from genomic DNA of LTR-tat3 transgenic mouse; Lane B contains PCR product of wild-type mouse DNA with the same specific primers; Lane C is the positive control with pHIV/LTR-tat3 plasmid as PCR template; lane D is the negative control of PCR because this reaction lacked DNA template; Lane E contains the size markers (100 bp ladder (GIBCO)). One of the bands in lane A has the same size (~750 bp) as the positive control pHIV/LTR-tat3 (lane C).

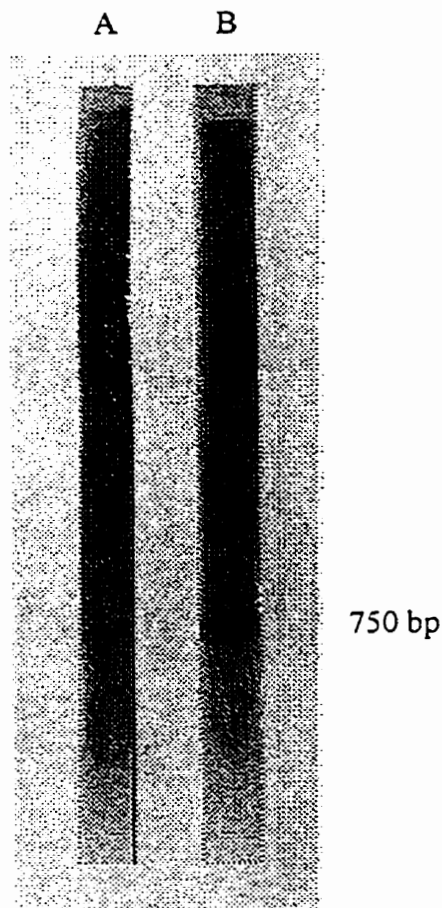


Fig.8: Southern blot of the PCR amplified LTR-tat3 insert.

Lane A contains the PCR products amplified from genomic DNA of LTR-tat3 transgenic mouse; lane B contains the positive control-PCR product from pHIV/LTR-tat3. Both lanes show a 750 bp fragment that hybridizes to the specific DNA probe made based on the pHIV/LTR-tat3 plasmid.

tat3. It was important to determine the size of the vector sequence flanking the LTR-tat3 in the integration site because the amplified adjacent mouse genomic sequences should be longer than the vector part in between. A 2kb fragment containing ~1kb LTR-tat3 plus ~1kb plasmid sequence was cleaved with KpnI and BglI from 3.4kb pHIV/LTR-tat3 (Fig.1) and transferred into mouse genome to generate the original transgenic mouse [106]. The restriction sites and fragments of pHIV/LTR-tat3 cleaved with different endonucleases are shown in Fig.1 and 4. PvuII has a single site in the middle of LTR-tat3 (500bp site); KpnI has a single site in the upstream region of LTR-tat3; BglI cleaves the pHIV/LTR-tat3 into 2 fragments: one is about 1150bp, the other is about 2240bp containing LTR-tat3. The shorter fragment of 500bp in length (in lane B) is the same length as the fragment between the upstream end of LTR-tat3 and the PvuII single site (500bp), indicating KpnI site is immediately in the upstream end of LTR-tat3. On the other hand, the 1.5kb PvuII/BglI fragment containing the 550 bp of LTR-tat3 part (in lane D) has an approximately 950 bp vector flanking sequence, which is between the tat3 and the mouse genomic DNA.

### **III. Inverse PCR (IPCR):**

Mouse genomic DNA was cleaved by a restriction endonuclease (SacII, BclI, or NcoI) and ligated using a low DNA concentration of 3ng/ul thereby favoring recircularization. These 3 types of circularized DNA were then purified and PCR amplified with two outward-reading primers (Lt150, Lt878) as shown in Fig.2. The PCR products from the 3 types of circularized DNA templates were shown in Fig.9. Each of the 3 types

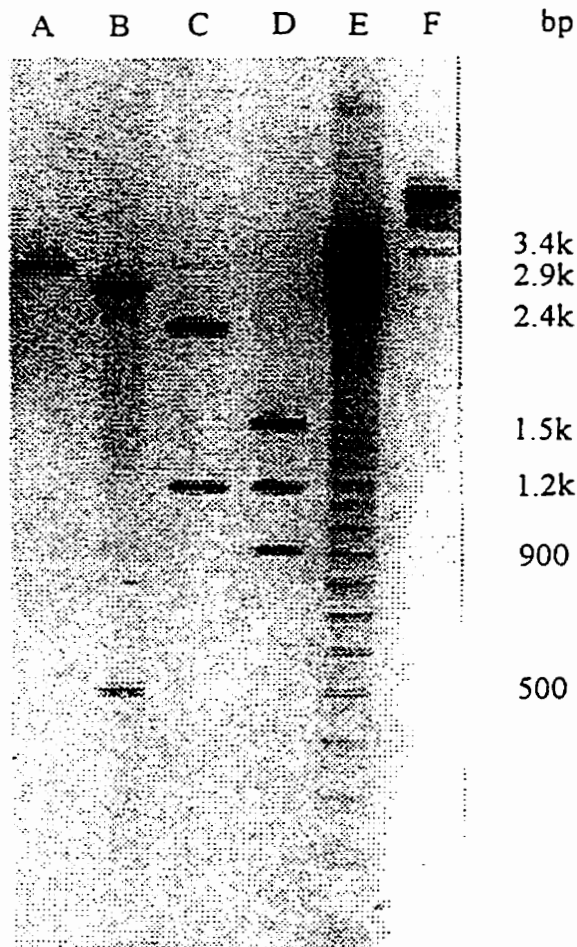


**Fig.4: Determination of the length of flanking segments (KpnI site-left end of LTR; right end of tat3-BglII site) of LTR-tat3 insert in vector pML.**

Lane A contains the Kpn I digest of pHIV/LTR-tat3; Lane B contains KpnI/PvuII double digest of pHIV/LTR-tat3; Lane C contains BglII digest of pHIV/LTR-tat3; Lane D contains BglII/PvuII double digest of pHIV/LTR-tat3; Lane E and F contain 100 bp DNA ladder and λHindIII digest, respectively.

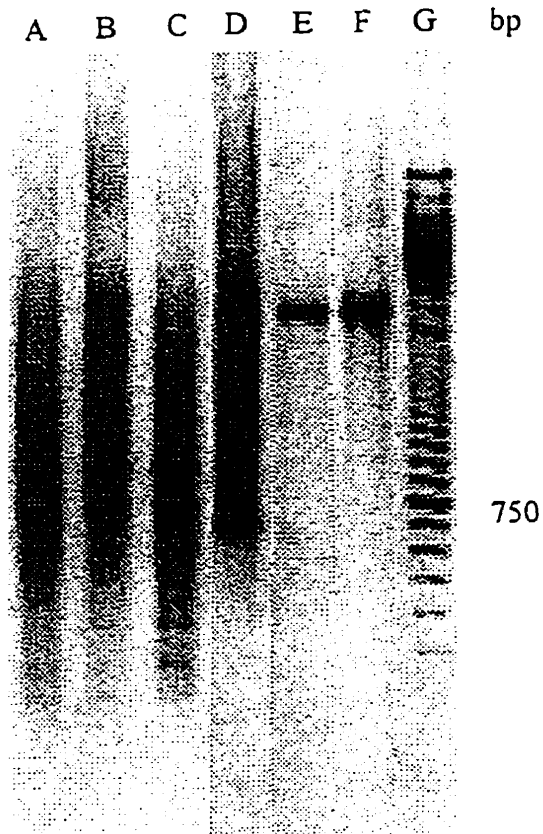


**Fig.9: Inverse PCR of LTR-tat3 transgenic H2 mouse DNA**

IPCPCR was performed with inverse primers based on LTR-tat3 as previously described. DNA was digested with a restriction enzyme and circularized by ligation, then used as IPCPCR template. Lane A, B, and C contain template DNA digested with SacII, NcoI, and BclI, respectively. Lane D contains the PCR amplified product from pHIV/LTR-tat3. Lane E contains the positive control for ligation: pHIV/LTR-tat3 digested with PstI that was re-circularized and used as the IPCPCR template. Lane F contains the positive control for IPCPCR : pHIV/LTR-tat3 used as DNA template. Lane G contains the size markers (100 bp DNA ladder).

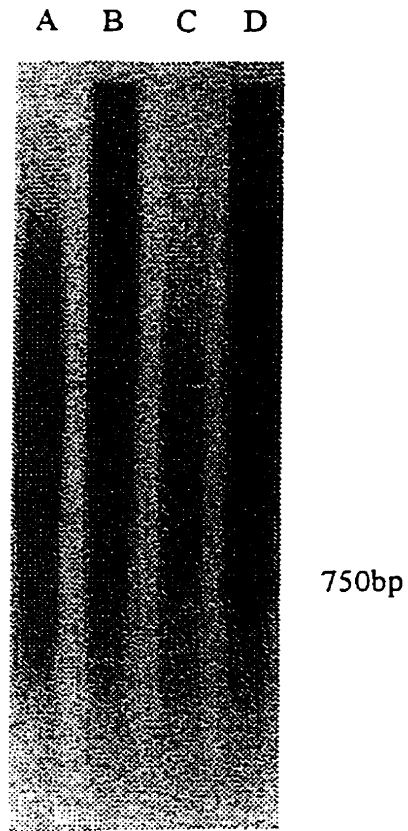


Fig. 10: Southern blot analysis of IPCR products.

IPCR bands were probed with DNA probe specific to pHIV/LTR-tat3. Lane A,B and C are IPCR products of transgenic mouse DNA corresponding to lane A,B and C in Fig.9. Lane D is PCR-amplified LTR-tat3 from pHIV/LTR-tat3.

of DNA template yielded multiple bands instead of one band. The two bands with same size that are shown in Fig.9 lane E and F, were the PCR products of recircularized pHIV/LTR-tat3 cut with PstI and the original pHIV/LTR-tat3 with the same set of outward-reading primers as above. None of the 3 types of circularized mouse genomic DNA showed hybridization by Southern blot to the specific probe made by random priming with pHIV/LTR-tat3 as template (Fig.10). The PCR product of 750bp fragment obtained from pHIV/LTR-tat3 using a pair of inward-reading primers (Lt132, Lt896), was used as positive control of Southern blot analysis.

#### **IV. Arbitrary PCR (APCR):**

The left junction of the LTR-tat3 insert was arbitrarily PCR amplified using a panel of conditions derived from the PCR Optimizer kit as shown in Table 3. In order to find the optimal condition to amplify the target sequence (i.e. The flanking mouse segment), each PCR reaction was carried out with the specific primer (11-mer LTR/L-2) and one arbitrary primer (10-mer OPA) from the 20 arbitrary primers. The specific primer LTR/L-2 was designed to have length similar to the arbitrary primer OPA in order to match the  $T_m$  of the two primers as much as possible. The annealing temperature of LTR/L-2 was optimized at 40°C as shown in Fig.11, whereas the arbitrary primers OPA were found to have a lower optimal annealing temperature at 36°C (Fig.11 and 12), which was also suggested by the kit supplier. Therefore, the annealing temperature was set at 40°C for the initial 5 cycles of primer extension, which was in favor of the LTR/L-2 annealing, and 36°C for the later PCR amplification, which

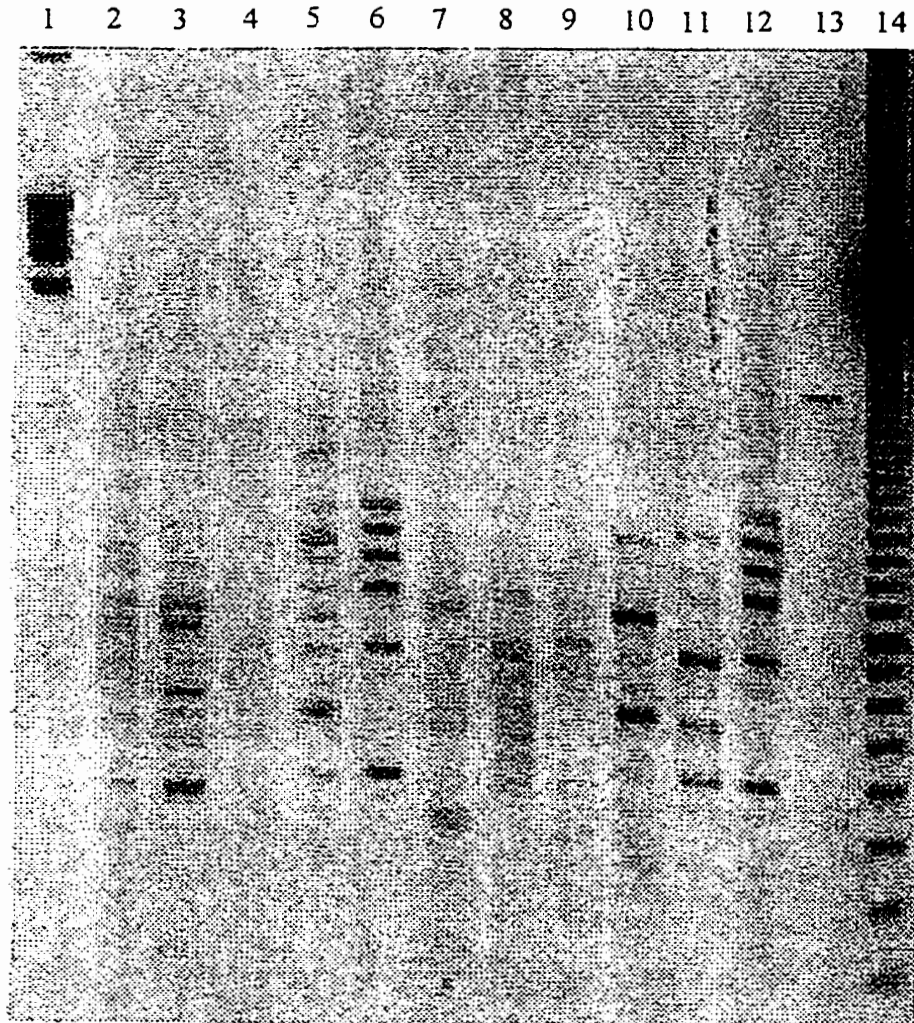


Fig. 11: Arbitrary PCR of left junction of LTR-tat3 transgene.

Lanes 2-11 contain PCR products with OPA 1 to OPA10; lane 12 is APCR with the single specific primer LTR/L-2; lane 13 is the positive control with pHIV/LTR-tat3 KpnI/BglI fragment; Lanes 1 and 14 contain the  $\lambda$ Hind III digests and the 100 bp DNA ladder. The optimal PCR annealing temperature is at 40°C; PCR pH = 9.0; [MgCl<sub>2</sub>]=2 mM.

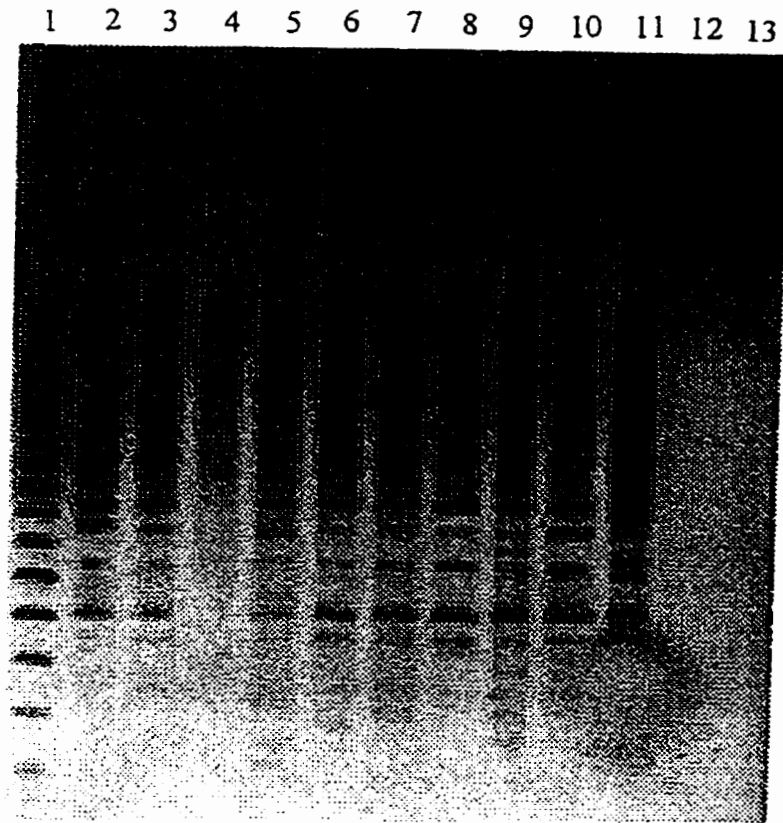


Fig.12: Arbitrary PCR of left junction of LTR-tat3 insert with arbitrary primers (OPAs) and specific primer LTR/L-2.

Lanes 2-11 contain PCR products with OPA11 to OPA20; lane 12 is the positive control with pHIV/LTR-tat3 KpnI/BglI fragment; Lanes 1 and 13 contain the 100 bp DNA ladder and the  $\lambda$ HindIII digest. The optimal PCR annealing temperature is at 40°C. PCR pH=9.0; [MgCl<sub>2</sub>]=2mM.

facilitated the annealing of both primer. The gel electrophoresis analysis shows that in each PCR condition, each pair of primers (the specific and an arbitrary primer) produce multiple bands and all the PCR products produced by the 20 pairs of primers share some common bands. This banding pattern will be discussed in the “Discussion” section. Of the 20 arbitrary primers, under these various PCR conditions, seven arbitrary primers at different pHs and MgCl<sub>2</sub> concentrations amplified 750-1100 bp DNA fragments that could hybridize to the specific probe made by random priming of the pHIV/LTR-tat3 kpnI/BglI fragment as template. This indicates that these positive bands shown in the Southern blot analysis (Fig.16) are potentially the mouse genomic sequences of interest. The optimal pH and MgCl<sub>2</sub> concentration for arbitrary primer (OPA1) were 9.0 and 2.5 mM respectively (Fig. 14); for OPA4 and 9, they were 8.5 and 2 mM respectively (Fig. 13); for OPA14,15, and 18, they were 9.0 and 2mM respectively (Fig.12); and for OPA20, they were 8.5 and 2.5mM respectively (Fig. 15).

Several stronger positive bands produced by OPA4, 9, 14, 15 and 18 were cut out from the gel, purified with the Genclean II kit (BIO/CAN Scientific, Mississauga, Ont.) and PCR amplified with the same primers as used for previous reactions. As shown in (Fig.19), all the bands can be re-amplified, confirming that the positive bands in Southern blot hybridization were specific fragments.

## **V. TAIL-PCR:**

Various conditions including reaction conditions and thermal-cycler conditions were tested to determine the optimal PCR conditions for the right-junction amplification.

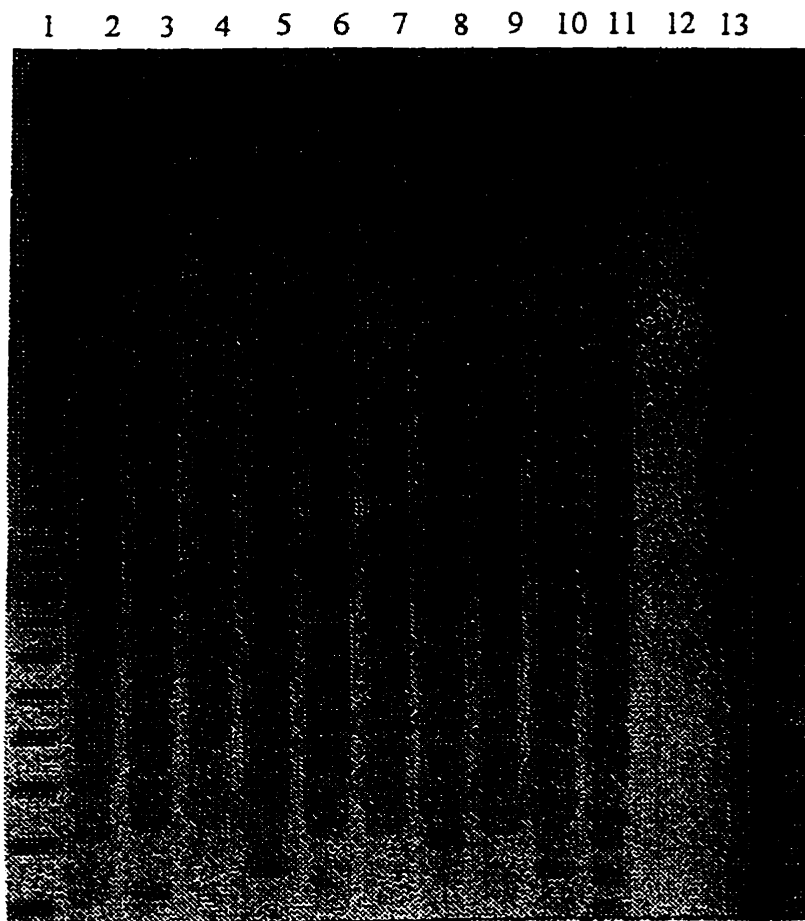


Fig.13: Arbitrary PCR of left junction of LTR-tat3 insert with arbitrary primers (OPAs) and specific primer LTR/L-2.

Lane 2-11 contain PCR products with OPA1 to OPA10; lane 12 is the positive control with pHIV/LTR-tat3 KpnI/BglI fragment; Lanes 1 and 13 contain the 100 bp DNA ladder and the  $\lambda$ HindIII digest. The optimal PCR annealing temperature is at 40°C. PCR pH = 8.5; [MgCl<sub>2</sub>] = 2mM.

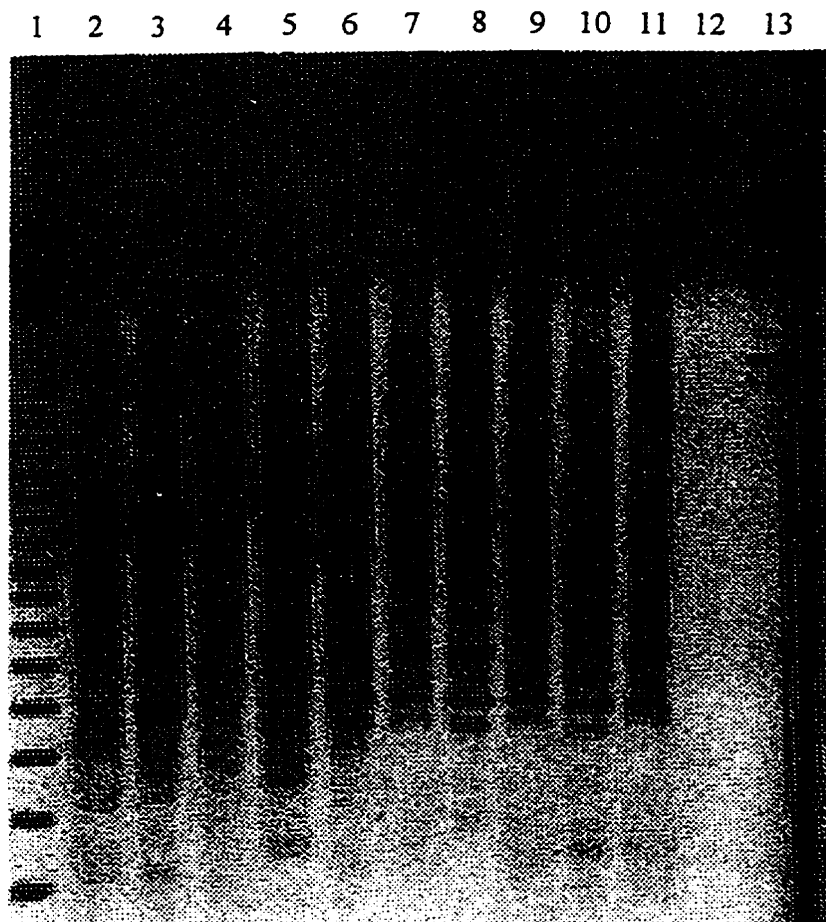


Fig.14: Arbitrary PCR of left junction of LTR-tat3 insert with arbitrary primers (OPAs) and specific primer LTR/L-2.

Lanes 2-11 contain PCR products with OPA1 to OPA10; lane 12 is the positive control with pHIV/LTR-tat3 KpnI/BglI fragment; Lanes 1 and 13 contain the 100 bp DNA ladder and the  $\lambda$ HindIII digest. The optimal PCR annealing temperature is at 40°C. PCR pH = 9.0; [MgCl<sub>2</sub>] = 2.5 mM.

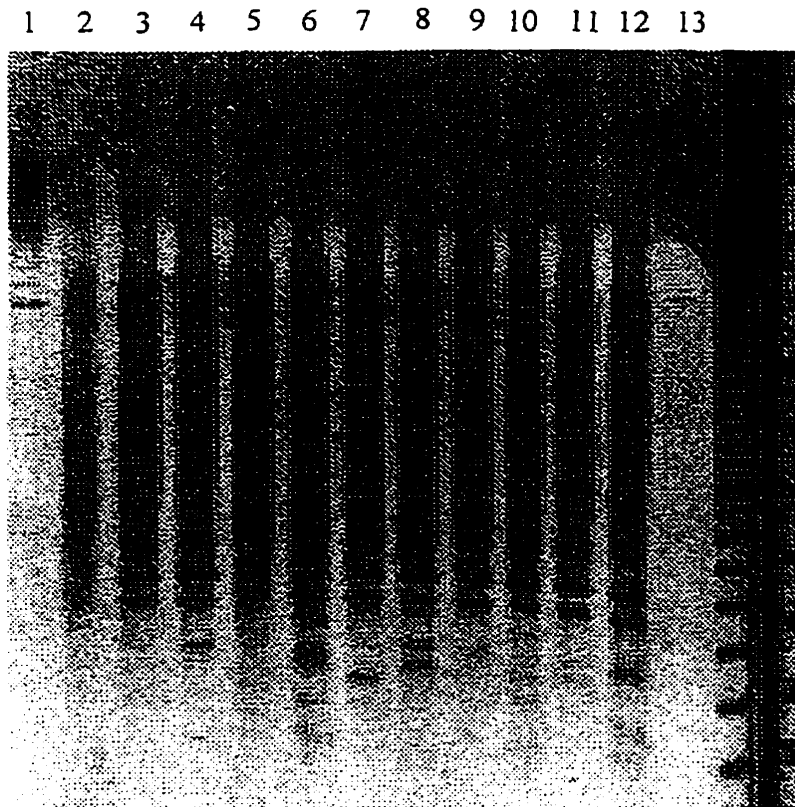


Fig.15: Arbitrary PCR of left junction of LTR-tat3 insert with arbitrary primers (OPAs) and specific primer LTR/L-2.

Lanes 2-11 contain PCR products with OPA11 to OPA20; lane 12 is the positive control with pHIV/LTR-tat3 KpnI/BglII fragment; Lanes 1 and 13 contain the 100 bp DNA ladder and the  $\lambda$ HindIII digest. The optimal PCR annealing temperature is at 40°C. PCR pH = 8.5; [MgCl<sub>2</sub>] = 2.5 mM.

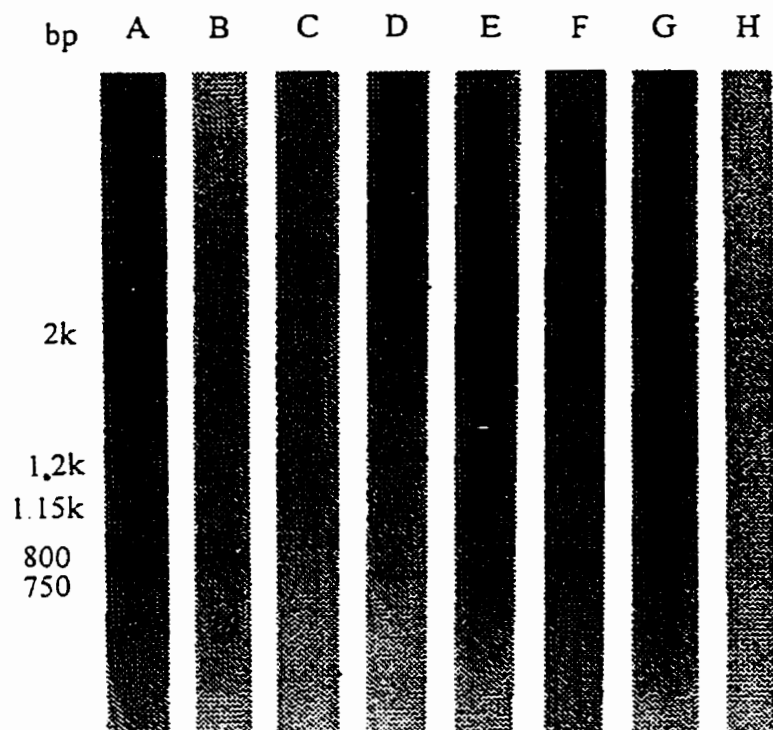


Fig.16: Southern blot analysis of arbitrary PCR products.

The APCR products were probed with LTR-tat3 specific DNA probe. Lane A, B, C, D, E, F, and G contain the APCR products with arbitrary primer OPA1, OPA4, OPA9, OPA14, OPA 15, OPA 18, and OPA20, respectively. Lane H is the positive control for Southern blot with 5 ng KpnI/EgII fragment of pHIV/LTR-tat3.

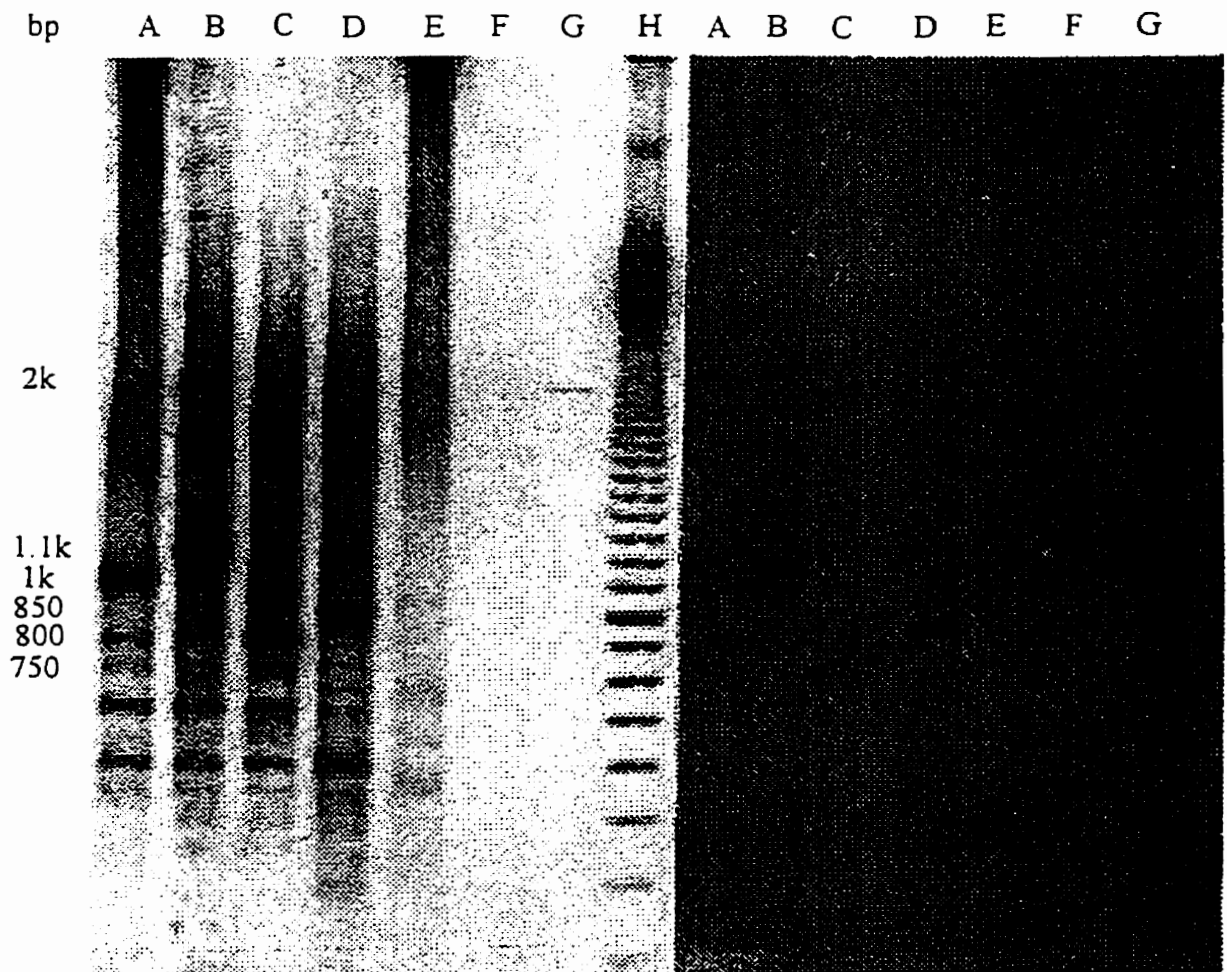


Fig.19: Re-PCR agarose gel analysis (left) and Southern blot analysis (right) of gel-purified positive APCR products with the same set of primers.

Lane A contains the PCR product of gel-purified 1000 bp fragment with OPA14; Lane B contains the 1100 bp fragment with OPA15; Lane C contains the 750 bp fragment with OPA15; Lane D contains the 800 bp fragment with OPA18; Lane E contains the 850 bp fragment with OPA4; Lane F contains with OPA9; lane G is the positive control for Southern blot with 5ng KpnI/BglI fragment of pHIV/LTR-tat3; Lane H is the 100 bp DNA ladder marker.

With the optimal condition listed in Table 4, all the PCR products produced by the 4 arbitrary primers exhibited various banding pattern (Fig.17). In primary TAIL-PCR, specific products may not always be amplified to detectable levels and also some non-specific products may be produced, therefore, some of the PCR products using the SP1 primer appeared as a “smear”. However, distinct bands did appear visible in the secondary and tertiary reactions. Some bands disappeared after the secondary TAIL-PCR using SP2 primer, indicating that these bands were nonspecific products. Some “novel” bands became visible in the tertiary PCR reaction using SP3 primer, implying that these bands could be specific products because they have undergone all the 3 nested primer annealing cycle. Fig.18 shows the Southern blot hybridization of the secondary and tertiary TAIL-PCR products with LTR-tat3 specific DNA probe. Of the 4 AD primers, only AD1 primer gave a strong band in the tertiary PCR reaction. This fragment is ~1100 bp in size which could contain ~150 bp sequences beyond the BglI site (right end) of the transgene fragment (Fig.1 and 5). This 150 bp segment could be the mouse flanking sequence.

This “Southern blot positive band” of 1100 bp and one “Southern blot negative” band produced with AD2 primer, used as negative control, were cut out, gel-purified using GeneClean II kit and subjected to an additional tertiary PCR amplification. Both bands can be re-amplified with the individual pair of primers, as shown in the agarose gel electrophoresis and Southern blot analysis in Fig.20, confirming that the 1100 bp fragment contained LTR-tat3 sequence.

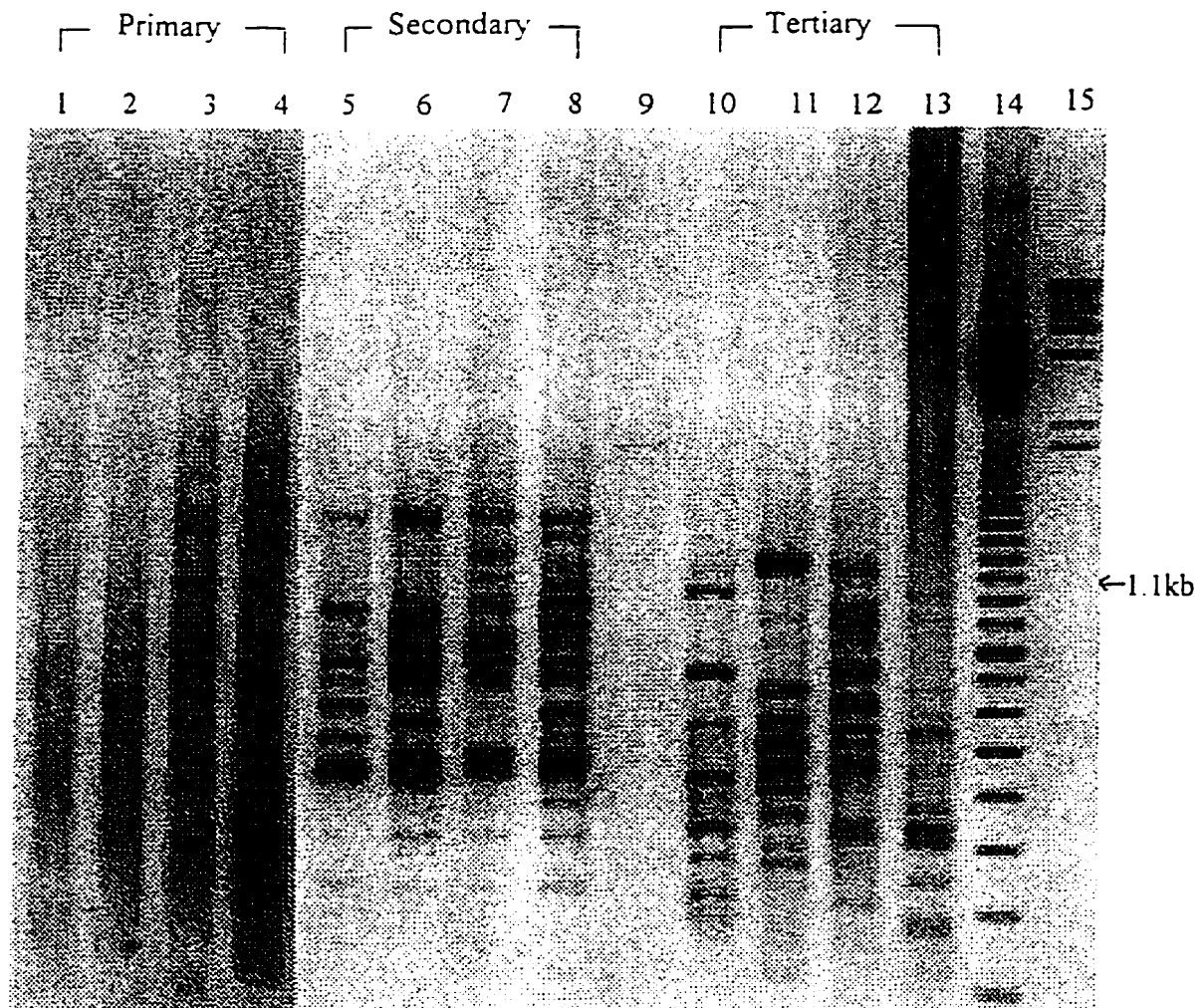


Fig. 17: TAIL-PCR of right junction of LTR-tat3 transgene.

PCR was performed as previously described. Lanes 1-4 contain the primary PCR products with arbitrary primers AD1-4 in order; Lanes 5-8 contain the secondary PCR products with AD1-4; Lanes 10-13 contain the tertiary PCR products with AD1-4; Lane 9 is the positive control with pHIV/LTR-tat3 *kpnI/BglII* fragment (5ng); Lanes 14 and 15 contain the 100 bp DNA ladder and the  $\lambda$ HindIII digest marker, respectively.

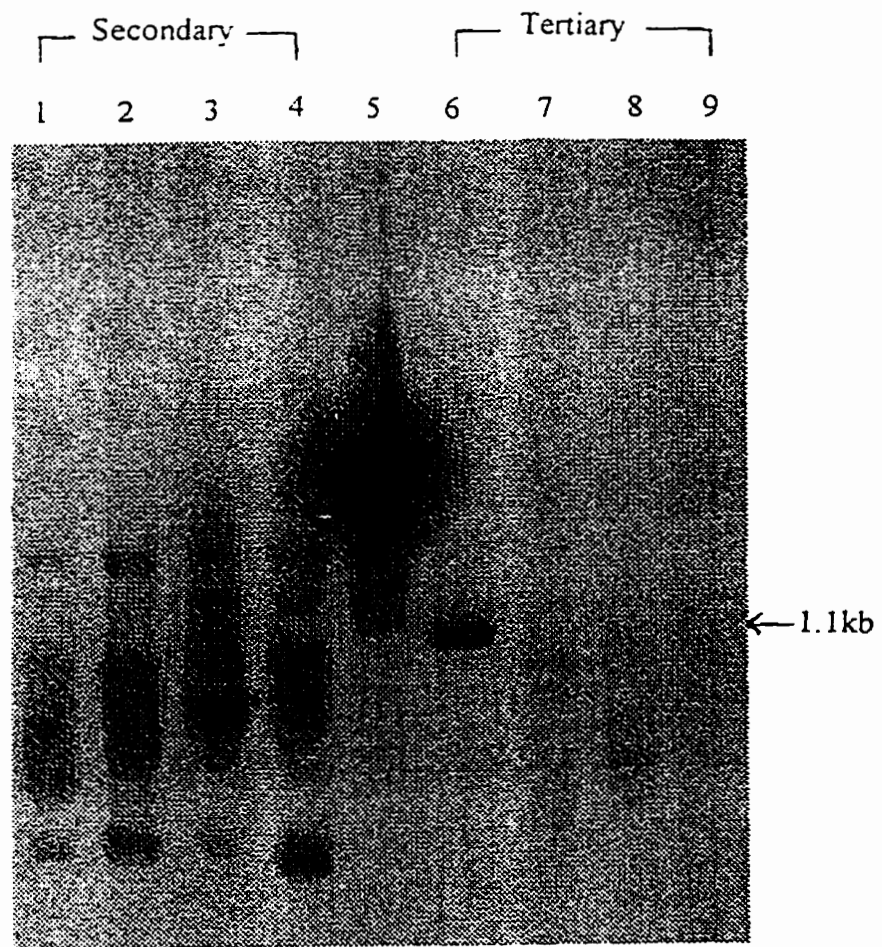


Fig.18: Southern analysis of TAIL-PCR products.

Lanes 1-4 contain the secondary PCR products with arbitrary primers AD1-4; Lanes 6-9 contain the tertiary PCR products with AD1-4; Lane 5 is the positive control with pHIV/LTR-tat3 KpnI/BglI fragment (5ng). Southern blot was probed with the probe specific to LTR-tat3 sequence.

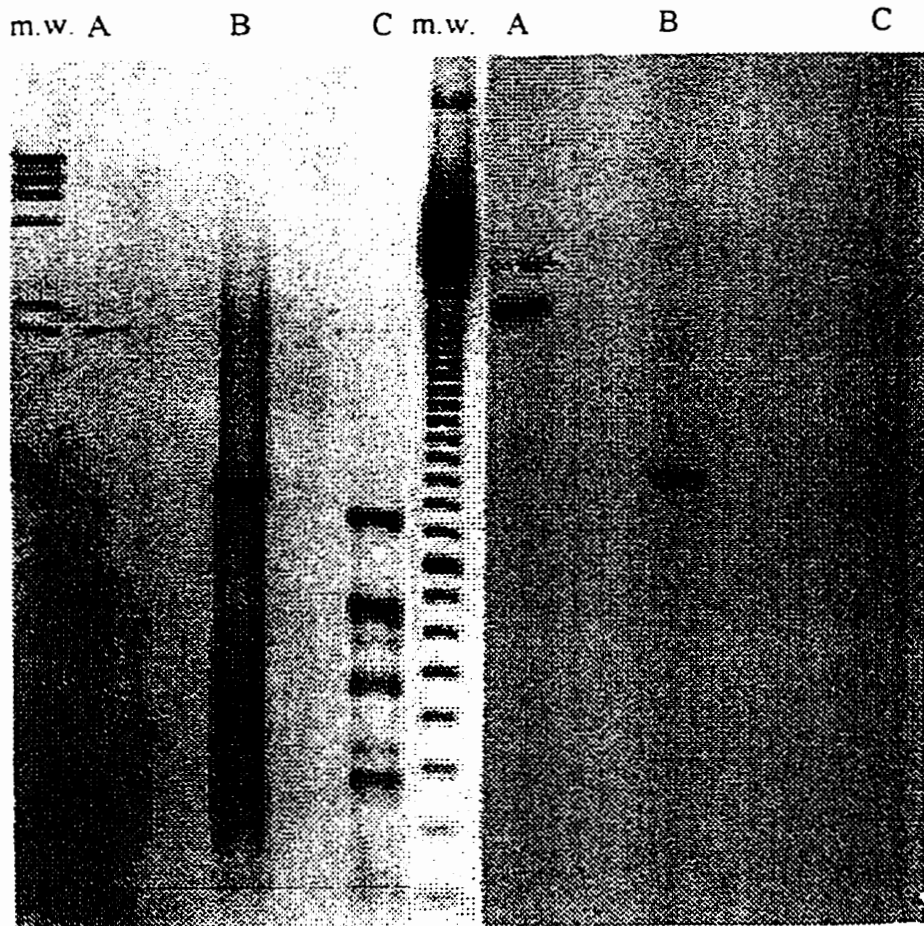


Fig.20: Confirmation of TAIL-PCR product with AD1 by gel (left) and Southern blot (right) analysis.

Lane A is the positive control, LTR-tat3 KpnI/BglI fragment; Lane B is TAIL-PCR product with arbitrary primer AD1; Lane C is the negative control, containing TAIL-PCR product using AD2, which did not hybridize to the LTR-tat3 specific probe; MW is the  $\lambda$ HindIII digest and the 100 bp DNA ladder.

## **VI. Sequencing analysis of the “Southern blot positive” DNA fragment**

The 1100 bp DNA fragments were sequenced with the specific primer SP3 or the arbitrary primer AD1 by a automatic sequencer (ABI PRISM). The results were shown in Fig.21 and 22. Both sequencing attempts terminated before reaching 450 bps, which is a typical sequence length for the automatic sequencer, and there are some unreadable nucleotides (N) in the two sequences generated. The sequence information is not adequate to make a solid conclusion, and this will be addressed in the Discussion section.

1	CGGAGANGAA	NNAGACGANN	AGGNGTGACA	GNAGGTAACN	NCAANACNNN	NTTTTTGGGG	60
61	GACAAACNNN	AAATTTTAGG	GGGGGAANCN	AANGNNAAN	TANACCCGAG	AGGAGNNAN	120
121	NANATAGCNA	NANNAGCAA	CNAACCNAAN	GANNACNGAC	AAAAANNNA	CAAGAGGCGA	180
181	ANNCACAAAN	ANCNANNACN	ANNNGANAC	AAAAGAAACA	AANAGNNNA	NGGANNAANA	240
241	AGAGNCANCG	CAGAGNNACN	AAANNCNANA	ANGAANNNNN	AAACAAAGNN	NGAAAAANAN	300
301	AAAAACCCAN	NNNTTTTNTC	NNCCNNNANN	NAAGNNNNAG	GAGCANAAGA	NAAAAANAAN	360
361	ACCNNCACTN	NANNTNANAA	CGAGNGAGAG	ANNAANCAA	AAGGNNACAG	NGNCNACGAA	420
421	ANNAACNCC	CCNANACGAC	AANCNNCCAA	ACNAAANNA	NNAGNANNNC	GAAAACNAAN	480
481	AGNAANCNAG	GAAANNAACN	CNAAAACCNA	NAAAAGAAA	GAGAACNAAN	ANGNAAANNA	540
541	NGNACAAAAN	NNAGAGTNAG	NANNNNCAAC	NCGAAGGACA	GAGAAAAGAG	AGAANNAAGN	600
601	CAGCAAAGAA	ANACAAAAAA	ANGAGAAACA	NACACGAANG	CAAAAGNCGC	AACAANGNAA	660
661	CNNGAAAAGN	AGCNAAGGNG	ANAAANANAA	AACNANCNAG	ACCNCAAGAG	AAAAANAAGN	720
721	GCANACCCNN	GAANGAANNN	NAACGTAAG				780

Fig.21. The sequence of the TAIL-PCR-amplified 1100 bp fragment with the specific primer SP3.

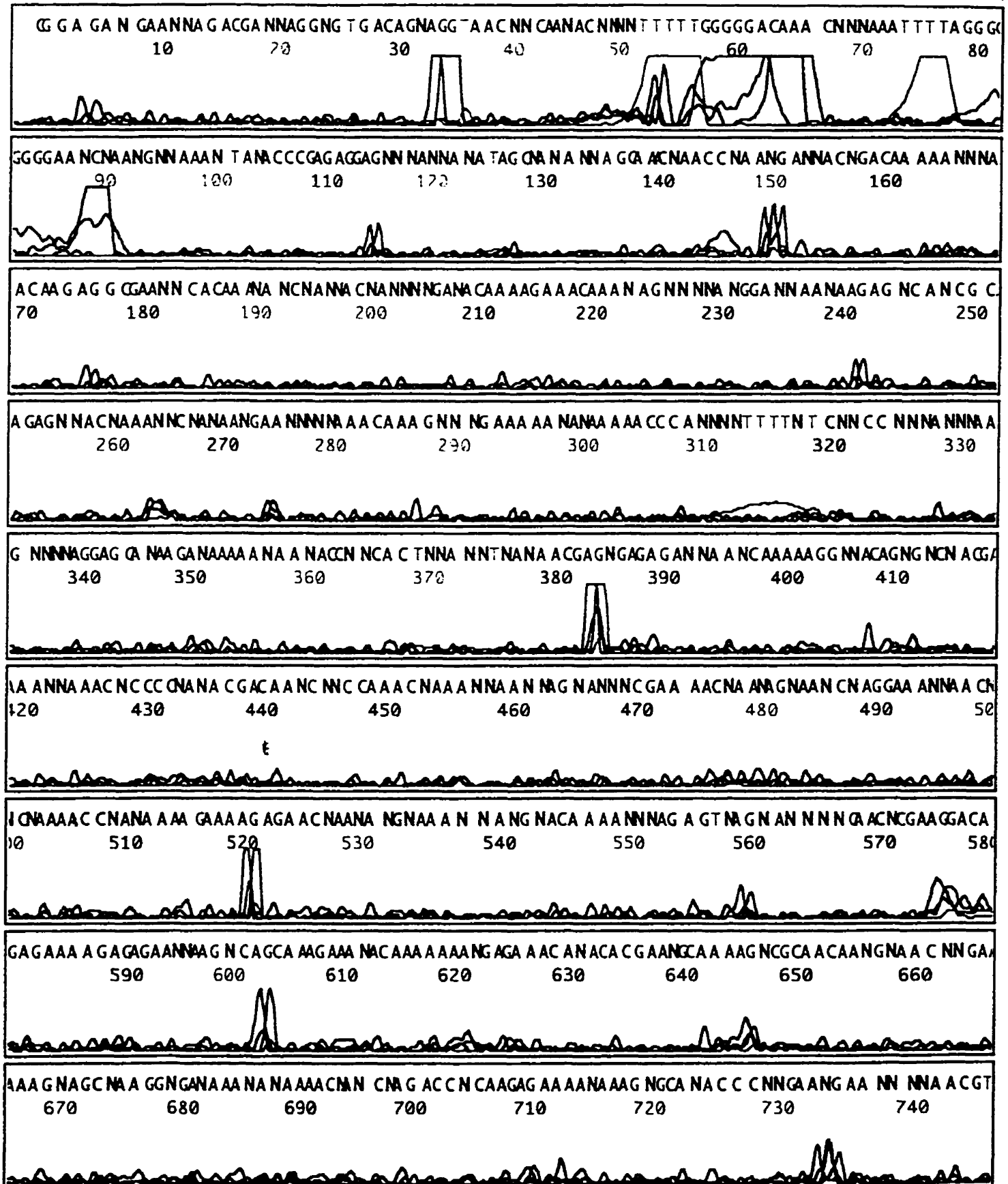


Model 310  
Version 3.0  
ABI-CE1  
Version 3.0

PY6Sample2/27/98  
PY6  
Lane 3

Signal G:34 A:25 T:62 C:32  
DT POP6(BD Set-Any Primer)  
dRhodPOP6  
Points 300 to 7080 Base 1: 300

Page 2 of 3  
Fri, Feb 27, 1998 6:03 PM  
Fri, Feb 27, 1998 5:06 PM  
Spacing: 12.00(12.00)



1	GNTTGNGGNA	AGACAAAGAT	ATNTGAGAGT	GAACCCGAGA	NTNNGATGGT	CGGTATTTAA	60
61	GACTGTATGG	TNCATGCTNC	ANACTATATT	CCTAGGGGCT	AGGACCAGTN	NTANCNTTAC	120
121	AGNCTATGGG	CTATCATAACA	NTAATGNATN	ACTTCNTATA	GTAATNCTAG	GATTNTAGAN	180
181	GCGNGATTGN	NNTNNNCANA	NTCANGANAC	NNAATGCTNT	NTTTTTTTTT	AGNAANGNTG	240
241	GNNANGGCNA	NCNNCCNAGN	TNNGGGNNNN	NTTNTNTCAN	NCGCCANANC	NTAANNANTA	300
301	ANNCCGCCN	CCAAAANATA	CCNCCCNNAN	AANATANNCA	TNTNTACACN	NNCTNNNNNN	360
361	NNCACNCCAN	NTCANNANTCA	ANTACNNAGN	CGTTNNACNA	AANANAANNA	AAGNNCNNNN	420
421	NANANNGTNG	CNNNNANCNT	NNAGCTTCCC	GCCNNGNNNN	NACAACCAAN	TANAGNCANA	480
481	ANNGTNNNCT	CANCNANAGA	NAANNANANC	NNAANNATNG	NGAANNANNC	TNANTNNACG	540
541	NGGAAAGCNN	NNGTNANCAN	CAANACNTNN	NACCGNNNGA	CNTNCTNNNA	NNNCNNNNGN	600
601	AAN						660

Fig.22. The sequence of the TAIL-PCR-amplified 1100 bp fragment with the arbitrary degenerate primer AD1.

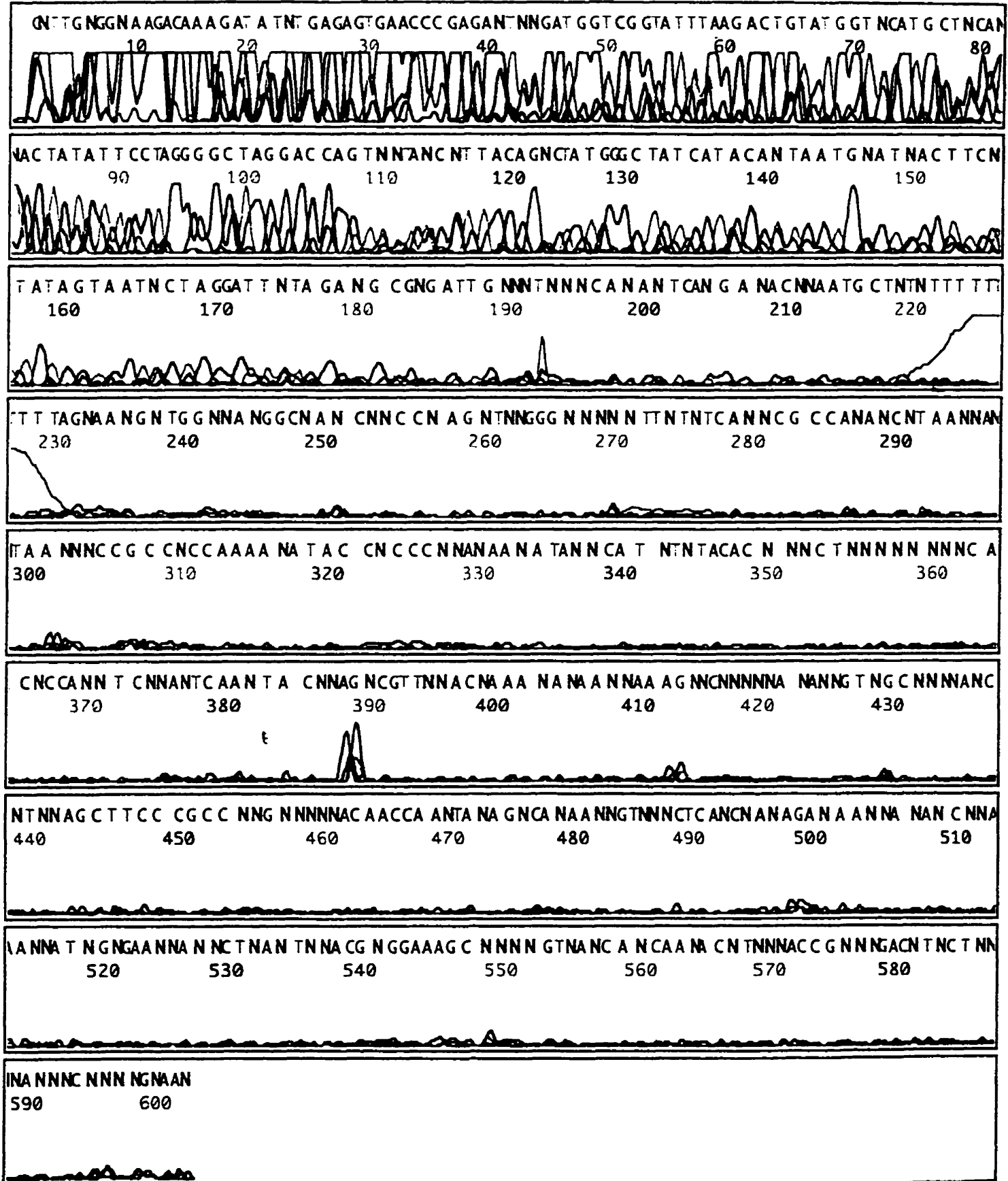


Model 310  
Version 3.0  
ABI-CE1  
Version 3.0

PY7Sample2/27/98  
PY7  
Lane 4

Signal G:112 A:77 T:189 C:104  
DT POP6(BD Set-Any Primer)  
dRhodPOP6  
Points 971 to 7080 Base 1: 971

Page 2 of 2  
Fri, Feb 27, 1998 7:01 PM  
Fri, Feb 27, 1998 6:03 PM  
Spacing: 11.63(11.63)



## Discussion

This study was undertaken to clone the mouse genomic sequence flanking the LTR-tat3 transgene in the obese transgenic mouse [106]. The flanking sequences of the transgene could be part of a potential gene responsible for the obese phenotype of this transgenic mouse. Various PCR strategies (inverse PCR, arbitrary PCR including TAIL-PCR) were applied to obtain mouse DNA sequences adjacent to the LTR-tat3 transgene. The transgene was detected by PCR amplification and subsequent Southern blot analysis confirmed the existence of the LTR-tat3 transgene in the obese mouse genome (Fig.5 and 6). This result was in agreement with the data provided by Dr. G. Jay who used a different strategy to detect the integration of the LTR-tat3 transgene. The genomic DNA was first digested with the restriction enzymes Bgl II (Fig.1), then subjected to Southern blot hybridization with the LTR-tat3 specific probe, revealing a 2kb fragment which is the length of the LTR-tat3 insert (including a part of the plasmid vector). The fact that the 2 kb band has the exact size of the LTR-tat3 insert and hybridized to the LTR-tat3 specific probe indicated that at least two copies of the LTR-tat3 insert may be integrated in a tandem array.

We made use of PCR cloning technology to isolate the DNA fragment flanking the transgene from the mouse genome without the necessity of generating a genomic libraries and isolating clones containing both the exogenous DNA and flanking sequences (81-83). The latter cloning method is more time-consuming and tedious.

There might be several factors involved in the failure of the inverse PCR approach to clone mouse genomic sequences adjacent to the LTR-tat3 transgene. We

assumed that the size of the exogenous DNA segment could be no less than 4 kb by virtue of the multiple copies of 2 kb LTR-tat3 transgene in the integration site as revealed by Southern blots. The length of the recognition sequence of SacII, BclI or NcoI is 6 nucleotides, meaning the cleavage frequency of the 3 restriction endonucleases is  $1/4^6$  bp  $\approx 1/4000$  bp in mouse genome. Theoretically there is one restriction site in every 4000 bp sequence in mouse genome for these endonucleases on average and the 3 endonucleases have no restriction site in the transgene. Therefore, the restriction digested mouse DNA fragment is estimated to be at least 8 kb. The large size of such a DNA fragment does not favor the efficient self-ligation (circularization) compared to fragments that are shorter. This poor circularization occurs even if the ligation conditions have been optimized based on the reduction of DNA concentration to avoid the formation of DNA concatemers, and the exclusion of polyethylene glycol 8000(PEG8000) from the ligation buffer (PEG is a macromolecular exclusion molecule which favors intermolecular ligation). Another factor that might have contributed to the failure of IPCR was the size of the DNA sequence flanking the LTR-tat3 transgene. As mentioned above, the mouse DNA segment flanking the LTR-tat3 in the restriction digested DNA fragment was estimated to be 4 kb on average. For IPCR, the outward primers (Lt150, Lt878) were designed based on the LTR-tat3 sequence beyond which there is a vector sequence of ~1 kb in size. Therefore, the size of the mouse DNA sequence plus the vector sequence could be about 5 kb on average, which was too long for efficient PCR elongation with Taq polymerase. The IPCR products were shown as multiple bands (Fig.9), all of which are 1 kb or less, indicating that none of them contains mouse DNA sequence due to the existence of the 1kb vector sequence between

the LTR-tat3 sequence, based on which the two outward primers were designed, and the mouse DNA sequence. The multiple bands (Fig.9) could contain the PCR products of one downstream primer of one copy LTR-tat3 and one upstream primer of the adjacent copy of LTR-tat3. This type of products would be expected to be ~1 kb in size due to some vector sequences integrated with the LTR-tat3. If this was the case, the band should be able to hybridize to the specific DNA probe based on the pHIV/LTR-tat3 plasmid, but no band was found to hybridize to the probe in Southern blot hybridization. However, the PCR product of LTR-tat3 (lane D in Fig.10) also hybridized poorly indicating the inferior quality of the DNA probe made by random priming. The DNA probe was made by using the intact plasmid pHIV/LTR-tat3 (~3.4 kb) as template, which contains a 1.4 kb plasmid fragment in addition to the 2 kb LTR-tat3 transgene. The specificity of this probe was actually derived from the ~1 kb ampicillin-resistance plasmid sequence downstream of the tat3 sequence. This means that only 1/3 of radioactive DNA fragments made by random priming was relevant for the detection of candidate PCR products. Although the reduced amount of the specific radioactivity can not lead to complete negative hybridization, it may contribute to some extent. Therefore, the KpnI/BglI fragment of pHIV/LTR-tat3 instead of intact plasmid was used as template for making probe in the subsequent experiments to increase hybridization efficiency.

The multiple bands shown in the gel analysis (Fig.9) could also be products from primer mispriming which led to the amplification of non-target sequences. This may occur in the IPCR reaction, because the amount of genomic DNA used was 1.4 ug that was much higher than the amount (100-200ng) commonly used for genomic DNA

PCR amplification. The large amounts of DNA provided more chances for mispriming to non-target sequences via non-specific binding. However, the products due to false priming were screened out by Southern hybridization because they did not hybridize to the specific probe (Fig.9 and 10).

Such inherent factors as DNA fragment size, the size of the flanking mouse DNA sequence and the tandem-linking nature of the LTR-tat3 transgene could account for the reduced efficiency of the IPCR method. The arbitrary PCR approach was then evaluated. In this approach, a set of arbitrary primers that bind to some non-specific sites, together with a specific primer complementary to the LTR-tat3 sequence were used to amplify the mouse DNA sequences flanking the LTR-tat3 gene. This approach showed generates a template for PCR, thereby facilitating the PCR cloning of the mouse DNA that is adjacent to the LTR-tat3 integration site.

Several PCR products that hybridized to the LTR-tat3 probe were obtained from transgenic mouse DNA using the arbitrary PCR approach (including TAIL-PCR). There are two possibilities for the positive bands that hybridized to the LTR-tat3 specific probe. One possibility is that they could be the potential mouse target sequences that flank the transgene. The other possibility is that they may be part of the LTR-tat3 transgene itself by virtue of the multiple copies of the LTR-tat3 gene in a tandem array as revealed in Southern blot analysis. The specific primers would anneal to the complementary sequences in each copy of the LTR-tat3 and the arbitrary primers could anneal to a certain place within the insert. A schematic diagram illustrating this possibility is shown in Fig.3. The second possible event could occur because the arbitrary primers can anneal to any complementary DNA sequence throughout the

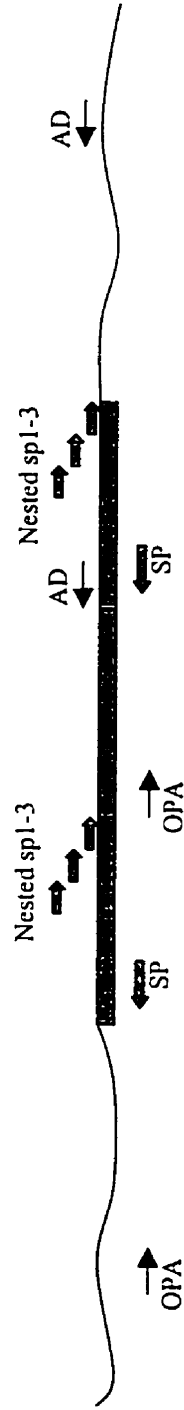


Fig.3: LTR-tat3 integration in tandem array.

The 3 nested specific primers SP1-3 binding to poly-complementary sequences of LTR-tat3 with arbitrary degenerated primers (AD) can produce PCR product within the LTR-tat3 insert by TAIL-PCR. The SP primer with the arbitrary primer OPA can do the same.

mouse genome including the LTR-tat3 transgene. Therefore, it is reasonable to infer that the positive PCR products may contain the mouse genomic DNA sequences flanking the LTR-tat3 transgene, however, the possibility of containing the LTR-tat3 sequences within the transgene can not be ruled out. Sequence identity will be discussed in a later section.

PCR amplification using mouse genomic DNA, which contains both target sequence and many irrelevant sequences, as the template can produce multiple bands due to mispriming of the primers to an irrelevant sequence which may have complementary segment to the primers in a non-optimal (low stringent) PCR condition. Furthermore, according to Liu's work [85], an arbitrary PCR reaction with one specific primer and one arbitrarily designed primer can result in more complicated PCR products that can be classified into 3 types: type I, those primed by the specific primer and arbitrary primer; type II, those primed by the specific primer alone; type III, and those primed by the nonspecific primer alone.

Type I PCR products include both specific products and nonspecific products that arise from mispriming. Only the specific type I PCR products will provide the target sequence that is the mouse genomic flanking sequences of the transgene insert. Type II and type III products are nonspecific.

In our study, all the agarose gel analysis of the arbitrary PCR products (for the left-junction) have shown a common banding pattern which was predicted as type II PCR products, produced by single specific primer mispriming. This common pattern is expected because the specific primer is shared by all PCR reactions while having different arbitrary primers. PCR amplification using the specific primer (LTR/L-2)

alone was attempted to verify the prediction. As shown in Lane 12 of Fig.11, the same multiple banding pattern was derived from a single primer PCR amplification. However, type II products as well as any nonspecific products of type I can be eliminated by carrying out successive reactions with nested specific primers as applied in TAIL-PCR (for the right-junction), as illustrated in Fig.5.

Type III products that are the major source of background produced by the nonspecific primer alone, can not be eliminated with nested specific primers, but can be reduced by thermal asymmetric PCR cycling. This also explained why the majority of product bands in the tertiary PCR reaction with the innermost specific primer and an AD primer did not hybridize to the LTR-tat3 specific probe in Southern blot analysis.

TAIL-PCR is a more efficient PCR approach that overcomes the shortcomings of existing PCR methods and it appears to favor the production of specific products [85]. The TAIL-PCR strategy is designed to favor amplification of the desired specific products of type I and suppress amplification of all the nonspecific products through thermal asymmetric PCR cycling, the use of nested specific primers plus a shorter arbitrary degenerate primer, and dilution of the previous round of PCR products to minimize the undesired products arising through mispriming. The key point is that the nested specific primers are purposely designed to be longer than the arbitrary degenerate (AD) primer which has a lower  $T_m$  (melting temperature) than that of the specific primers. This provides the basis for the interspersed high-stringency PCR cycling which favors the efficient longer specific primer annealing to the DNA template, with reduced-stringency PCR cycling which facilitates both specific and AD primers annealing to the template. TAIL-PCR begins with high-stringency cycling so as

to enrich the target segment flanking LTR-tat3 transgene that can then undergo subsequent efficient amplification. Likewise, for the arbitrary PCR of the left-junction, enrichment of the left adjacent target sequence was achieved by starting with single specific primer extension before PCR amplification. One low-stringency PCR cycle following the high-stringency cycling was designed to maximize AD primer annealing within the target sequence together with the specific primer to amplify the target sequence.

The typical automatic sequencing normally produces about 450 nucleotides. The result from the sequencing analysis of the “Southern hybridization positive” DNA fragment revealed a prematurely terminated nucleotide strand and many nucleotides whose signals were unrecognizable by the automated sequence detection. There are several possible explanations. Firstly, the primer for sequencing is better to be nested by the original primer that generates the DNA template used in the sequencing analysis. The nested sequencing primer has an indented priming site in the DNA template, which facilitates the primer binding to the DNA template and in turn increases the sequencing efficiency. Secondly, the primer used for sequencing needs to be of high-purity and the routine PCR primers used in our study may not have been adequate for this automated sequencing approach because the components of the impure primer preparation can inhibit the sequencing reaction. In addition, excessive degraded primers also can result in sequencing problem due to the inefficient priming. Thirdly, DNA template purity is also needed for a good sequencing result. The DNA fragments used in this study for sequencing were gel-purified with GeneClean II kit. Theoretically, gel-purified DNA should be adequate for sequencing, but the DNA preparation may be detrimentally

affected by poor quality of Kit reagents or improper handling. In addition, the ratio of DNA template to the primer used is also a determining factor. Finally, the PCR fragments have undergone about 80-90 cycles of PCR reactions in all, which might have led to increased mutation frequency. The lack of homogeneity of the DNA fragment that was used as template for sequencing might also cause sequencing problems. The search performed for the homology between the sequence of the 1100 bp fragment and the LTR-tat3 insert sequence (pHIV/LTR-tat3 Kpn I/Bgl I fragment) has not provided any meaningful information due to many "N"s (non-recognizable nucleotide signal) among the nucleotides and the limited known sequence of the 1100 fragment.

Sequence analysis of the genomic sequences flanking LTR-tat3 transgene is necessary to determine the identity of this gene. The DNA sequence of the PCR products that hybridized to the LTR-tat3 probe could then be used to search the genbank database for any homologous sequences. If the fragment sequence is not long enough to provide enough information for gene identification, further chromosomal walking [109] using this known flanking sequence as the starting point would produce more sequence information for the candidate gene. Based on this flanking sequences of the LTR-tat3 transgene, a specific DNA probe could be made, and then used to screen a mouse genomic DNA library for a genomic DNA clone containing a complementary sequence to the probe. The cloned genomic DNA fragments could be subjected to "exon trapping" [87,88], based on the selection of RNA sequences (exons) which are flanked by functional 5' and 3' splice sites. Exon trapping will allow the identification of the

coding sequences of the potential gene. By using the approaches described, the whole potential gene interrupted by the LTR-tat3 transgene could be cloned and identified.

As far as we know, the tat protein has not been found to be directly or indirectly involved in energy metabolic regulatory pathways, and as mentioned in the “Introduction” section, only one out of six transgenic mice exhibited the obese phenotype apart from the Kaposi’s sarcoma-like skin lesions shared by all the six transgenic mice. Therefore, we assume it is the specific transgene integration event occurred in the obese H2 mouse that led to the obese phenotype. It is not possible to predict where the LTR-tat3 transgene in the chromosome will integrate after being transferred into the mouse fertilized eggs. However, retroviruses and other insertion elements show a remarkable preference for sites of integration. Some evidence strongly suggests [86] that transcriptionally active genome regions are preferred targets for retrovirus integration, indicating integration in the vicinity of a functional gene. Based on the fact [86] that the retrovirus insertion is much less random than expected, we could extrapolate that the transgene, especially with LTR of retrovirus HIV linked to the upstream of the gene, might probably integrate into some preferred chromosomal regions where certain chromosomal organization might exert its influence on the integration process. It is possible that the insertion of the LTR-tat3 transgene in a potential transcriptionally active genome region has disrupted a functional gene. Alternatively, the insertion of LTR, which is a transcription activator, led to an aberrant overexpression of an endogenous gene whose product is involved in energy metabolic pathway. This overexpressed protein result in a metabolic dysregulation—obese phenotype. While the work presented in this thesis did not come to the point of

identifying the potential gene, further work based on “Southern blot positive” DNA fragments obtained from this work could be done to identify and characterize the potential candidate obese gene or the genetic nature of the resulting obese phenotype of the transgenic mouse.

## References

- [ 1]: Sawaya AL. Dallal G., Solymos G., et al. Obesity and malnutrition in a shantytown population in the city of Sao Paulo, Buazil. *Obesity Res.* 1995,3: 107S-15S
- [ 2]: Keesey,R.E.(1980). In *Obesity*, A.Stunkard, eds ( Philadelphia: W.B. Saunders Co.) pp. 144-166
- [ 3]: Harris, R.B.S.(1990). Role of et-point theory in regulation of body weight. *FESEB J.* 4, 3310-3318
- [ 4]: Bouchard, C. 1992, In *Obesity in Europe 91*. G. Ailhand et al.,Eds.: 2: 7-14
- [ 5]: Stunkard, A.J., T.I. A. Sorensen and C. Hanis. An adoption study of human obesity. *N. Engl. J.Med.* 1986, 314: 193-198
- [ 6]: Bouchard, C. and L. Perusse. Genetics of obesity. *Annu. Rev. Nutr.* 1993, 13: 1477-1482
- [ 7]: Bouchard,C., Tremblay, A., Nadeau, A., Despres, J.P., Theriault,G., Soulay, M.R.  
Genetic effect in resting and exercise metabolic rates. *Metabolism* 1989,38:364
- [ 8]: Roberts S.B., Greenberg A.S. The new obesity genes. *Nutr Rev* 1996, 54: 41
- [ 9]: Bouchard C. 1994. Genetics of obesity: overview and research directions. In: *The Genetics of Obesity* (Bouchard C., ed.),pp.223-233. CRC Press, Boca Raton, FL
- [10]: Yvon C. Chagnon, Familial aggregation of obesity, candidate genes and quantitative trait loci. *Curr Opin Lipidol.* 1997, 8: 205-211
- [11]: Leibel,R.L. Is obesity due to a heritable difference in “sit point” for adiposity?

West J Med 1990,153: 429-431

[12]: Greenberg, D.A. Linkage analysis of “necessary” disease loci versus “susceptibility” loci. Am. J. Hum. Genet. 1993, 52: 135-143

[13]: Bouchard, C. Perusse, L. 1988. Heredity and body fat. Annu. Rev. Nutr. 8:259-277

[14]: Leibel, R.L., Bahary, N., Friedman, J.M. Genetic variation and nutrition in obesity: approaches to the molecular genetics of obesity, in Genetic Variation and Nutrition, Simipoulos, A.P. and Childs, B., Eds, Karger Publishing, 1990

[15]: Friedman, J. and Leibel, R.L. Tackling a weighty problem. Cell 1992, 69:217(?)

[16]: Moll, P.P., Burns, T.L. Lauer, R.M. The genetic and environmental sources of body mass index variability: The muscatine ponderosity family study. Am. J. Hum. Genet. 1991, 49:1243-85

[17]: Price, R.A., Ness, R., LasKazewski, P. Common major gene inheritance of extreme overweight. Hum. Biol. 1990, 62:747-65

[18]: Province, M.A., Arnqvist, P., Keller, J., Higgins, M., Rao, D.C. Strong evidence for a major gene for obesity in the large, unselected, total community health study of Tecumseh. Am. J. Hum. Genet. 1990, 47(suppl): A143 (Abstr.)

[19]: Chagnon, Y.C., Bouchard, C. Genetics of obesity: advances from rodent studies.. Trends Genet. 1996, 12:441-444

[20]: Perusse, L., Chagnon, Y.C., Dionne, F.T. Bouchard, C. The human obesity gene map: the 1996 update. Obes. Res. 1997, 49-61

[21]: Chagnon, Y.C., Perusse, L. Suggestive linkages between markers on human

- 1p32-p22 and body fat and insulin levels in the Quebec family study. *Obes. Res.* 1997, 5, 115-121
- [22]: Lembergas, A.V., Perusse, L. Identification of an obesity quantitative trait locus on mouse chromosome 2 and evidence of linkage to body fat and insulin on the human homologous region 20q. *J. Clin. Invest.* 1997, 10, 166-173
- [23]: Nadeau, J. H. Linkage and synteny homologies between mouse and man. *The Jackson Laboratory*, 12, March, 1990
- [24]: Nadeau, J. H., M.T. Davisson, D.P. Doolittle, P. Grant, A.L. Hillyard, M. et al. Comparative map of mice and humans. *Mammal. Genome* 1991, 1: S461-S515
- [25]: Bouchard, C. Genetics of human obesity: recent results from linkage studies. *J. Nutr.* 1997, 127: 1887S-1890S
- [26]: Bouchard, C., Perusse, L. Current status of the human obesity gene map. *Obes. Res.* 1996, 4: 81-90
- [27]: Wilson, B.D., Ollmann M.M., Kang L., Stoffel M., Bell G.L., Barsh G.S. Structure and function of ASP, the human homolog of the mouse agouti gene. *Hum. Mol. Genet.* 1995, 4: 223-230
- [28]: Bultman, S. J., Michaud, E.J. Molecular characterization of the mouse agouti locus. *Cell.* 1992, 71: 1195-1204
- [29]: Lu, D. et al. Agouti protein is an antagonist of the melanocystimulating-hormone receptor. *Nature* 1994, 371: 799-802
- [30]: Peery W.L., Hustad C.M., Swing D.A., Jenkin N.A., Copeland N.G. A transgenic mouse assay for agouti protein activity. *Genetics* 1995, 140: 267-274

- [31]: Kleibig ML, Wilinon JG, Geisler JG, Woychik RP. Ectopic expression of the agouti gene in transgenic mice causes obesity, features of type II diabetes and yellow fur. Proc Natl Acad Sci Uci USA 1995,92: 4728-32
- [32]: Zemel MB, Han Kim J, Woychik RP, et al. Agouti regulation of intracellular calcium: role in the insulin resistance of viable yellow mice. Proc Natl Acad Sci USA 1995, 92: 4733-37
- [33]: Jones BH, Kim JH, Zemel MB, et al. Upregulation of adipocyte metabolism by agouti protein: possible paracrine actions in yellow mouse obesity. Am J Physiol 1996, 270: E192-E196
- [34]: Coleman DL, Eicher EM: Fat (*fat*) and tubby (*tub*) two autosomal recessive mutations causing obesity syndromes in the mouse. J Hered 1990, 88: 424-427
- [35]: Chagnon YC., Perusse L. Familial aggregation of obesity, candidate genes and quantitative trait loci. Curr. Opin. Lipidol. 1997, 8: 205-211
- [36]: Naggert, JK.,Fricker LD., Varlamov,O., Nishina, PM., Rouille Y. et al. Hyperproinsulinaemia in obese fat/fat mice associated with a carboxypeptidase E mutation which reduce enzyme activity. Nat. Genet. 1995,10: 135-142
- [37]: Nickells, RW., Schlamp, CL., Newton, AC., and Williams, DS. Gene expression of the neuropeptide-processing enzyme carboxypeptidase E in rat photoreceptor cells. J Neurochem. 1993,61: 1891-1900
- [38]: Noben-Trauth, K., Naggert, JK., North MA. And Mishina PM. A candidate gene for the mouse mutation tubby. Nature 1996, 380: 534-538
- [39]: Kleyn, PW., Wei Fan, Steve G., Kovats, John J.Lee. et al. Identification and

- characterization of the mouse obesity gene *tubby*: a member of a novel gene family. *Cell* 1996,85: 281-290
- [40]: Zhang, Y., Proenca, R., Maffei, M., Barone, M., Leopold, L. and Friedman, J. M. Positional cloning of the mouse obese gene and its human homologue. *Nature (London)* 1994, 372: 425-432
- [41]: Campfield, LA., Smith, FJ., Guisez, Y., Devos, R. and Burn, P. Recombinant mouse OB protein: evidence for a peripheral signal linking adiposity and central neural networks. *Science* 1995,269: 546-549.
- [42]: Halaas, JL., Gajiwala, KS., Maffei, M.,cohen, SL., Chait, BT., Rabinowitz, D., Lallone, RL., Burley, SK. And Friedman,JM. Weight-reducing effects of the plasma-protein encoded by the *obese* gene. *Science* 1995,269: 543-546
- [43]: Pelleymounter, MA., Cullen, MJ., Baker, MB., Hecht, R., Winters, D., Boone, T. and Collins,F. Effects of the *obese* gene-product on body weight regulation in *ob/ob* mice. *Science* 1995, 269: 540-543
- [44]: MacDougald, OA., Hwang, CS., Fan, H., and Lane, MD. Regulated expression of the *obese* gene product (leptin) in white adipose tissue and 3T3-L1 adipocytes. *Proc. Natl. Acad. USA* 1995, 92: 9034-37
- [45]: Sliker, L., Sloop, K., Surface, P., Kriaciunas, A., Laquier,F., Manetta., J., Buevallesey, J., and Stephens, T. Regulation of expression of OB mRNA proteins by glucocorticoids and cAMP. *J. Biol. Chem.* 1996,271:5301-04
- [46]: Mantzoros, CS., Qu, D., Frederich,RC., Susulic, V.S., Lowell, BB., Maratos-Flier, E., and Flier, JS. Activation of beta3 adrenergic receptors suppresses leptin

expression and mediates a leptin-independent inhibition of food intake in mice.

Diabetes 1996, 45: 909-914

[47]: Grunfeld, C., Zhao, C., Fuller, J., Pollack, A., Moser, A., Friedman, J., and Feingold, K.R. Endotoxin and cytokines induce expression of leptin, the *ob* gene product, in hamsters. J. Clin. Invest. 97, 2151-57

[48]: Considine, R.V., Considine, E.L., Williams, C.J., Nyce, M.R., Magosin, S.A., Bauer, T.L., Rosato, E.L., Colberg, J., and Caro, J.F. Evidence against either a premature stop codon or the absence of obese gene mRNA in human obesity. J. Clin. Invest. 1995, 95: 2986-88

[49]: Maffei, M., Stoffel, M., Barone, M., Moon, B., Dammerman, M., Ravussin, E., Bogardus, C., Ludwig, D.S., Flier, J.S., Talley, M., Auerbach, S., and Friedman, J.M. Absence of Mutations in the human OB Gene in Obese/Diabetic Subjects. Diabetes 1996, 45: 679-682

[50]: Niki, T., Mori, H., Tamori Y., Kishimoto-Hashimoto, M., Ueno, H., Araki, S., Masugi J., Sawant, N., Majithia, H.R., Rais, N., Hashiramoto, M., Taniguchi, H., and Kasuga, M. Molecular Screening in Japanese and Asian Indian NIDDM patients associated with obesity. Diabetes 1996, 45: 675-678

[51]: Clement, K., Garner, C., Hager, J., Philippi, A., LeDuc, C., et al. Indication for linkage of the human OB gene region with extreme obesity. Diabetes 1996, 45: 687-690

[52]: Reed, D.R., Ding, Y., Xu, W., Cather, C., Green, E.D., and Price, R.A. Extreme obesity may be linked to markers flanking the human ob gene. Diabetes 1996, 45: 691-

- [53]: Maffei, M., Halaas, J., Ravussin, E., Pratley, R.E., Lee, G.H., Zhang, Y., Fei, H., Kim, S., Lallone, R., Ranganathan, S., Kern, P.S., and Friedman, J.M. Leptin levels in human and rodent: Measurement of plasma leptin and ob RNA in obese and weight-reduced subjects. *Nature Med.* 1995, 1: 1155-1161
- [54]: Friedman, J.M., Leibel, R.L., Siegel, D.S., Walsh, J. and Bahary, N. Molecular mapping of the mouse ob mutation. *Genomics*, 1991, 11: 1054-1062
- [55]: Bahary, N., Siegel, D.A., Walsh, J., Zhang, Y., Leopold, L., Liebel, R., Proenca, R. and Friedman, J.M. Microdissection of proximal mouse chromosome 6: identification of RFLPs tightly linked to the ob mutation. *Mammalian Genome* 1993, 4: 511-515
- [56]: Tartaglia, L.A., Dembski, M., Weng, X., Deng, N., Culpepper, J., Devos, R., Richards, G.J. et al. Identification and expression cloning of a leptin receptor, OB-R. *Cell* 1995, 83: 1263-71
- [57]: Chen H, Charlat O, Tartaglia LA, et al. Evidence that the diabetes gene encodes the leptin receptor: identification of a mutation in the leptin receptor gene in db/db mice. *Cell* 1996, 84: 491-495
- [58]: Lee G-H, Proenca R, Montez JM, et al. Abnormal splicing of the leptin receptor in diabetic mice. *Nature* 1996, 379: 632-635
- [59]: Coleman, D.L. Obese and diabetes: two mutant genes causing diabetes-obesity syndromes in mice. *Diabetologia* 1978, 14: 141-148
- [60]: Ghilard, N., Ziegler, S., Wiestner, A., Stoffel, R. Heim, M.H., and Skoda, R.C. Defective STAT signaling by the leptin receptor in diabetic mice. *Proc. Natl. Acad. Sci.*

USA. 1996, 93: 6231-35

[61]: Mercer, JG., Hoggard, N., Williams, LM., Lawrence, CB., Hannah, LT., and Trayhurn, P. Localization of leptin receptor mRNA and the long form splice variant (Ob-Rb) in mouse hypothalamus and adjacent brain regions by in situ hybridization.

FEBS Lett. 1996, 387: 113-116

[62]: Billington, C.J., Briggs, J.E., Grace, M and Levine, A.E. Effects of intracerebroventricular injection of neuropeptide Y on energy metabolism. Am J Physiol 1991, 260: R321-R327

[63]: Egawa, M., Yoshimatsu, H. and Bray, G.A. Neuropeptide Y suppresses sympathetic activity to interscapular brown adipose tissue in rats. Am J Physiol 1990, 260: R328-R334

[64]: Williams, G., McKibben, P.E. and McCarthy, H.D. Hypothalamic regulatory peptides and the regulation of food intake and energy balance: signals or noise? Proc. Nutr. Soc. 1991, 50: 527-544

[65]: Stephens, T.W. et al. The role of neuropeptide Y in the antiobesity action of the obese gene product. Nature 1995, 377: 530-532

[66]: Schwartz, M.W. et al. Specificity of leptin action on elevated blood glucose levels and hypothalamic neuropeptide Y gene expression in ob/ob mice. Diabetes 1996, 45: 531-535

[67]: Bing, C., Wang, Q., Pickavance, L. and Williams, G. The central regulation of energy homeostasis: role of neuropeptide Y and other brain peptides. Biochem. Soc. Trans. 1996, 24: 559-565

- [68]: Chau, SC., Chung, WK., Wu-Peng, XS., Zhang, Y. Liu, S.-M. et al. Phenotypes of mouse diabetes and rat fatty due to mutations in the OB (leptin ) receptor. *Science* 1996, 271: 994-996
- [69]:Frankel, WN. Taking stock of complex trait genetics in mice. *Trends Genet.* 1995,11: 471-477
- [70]: Katz, EB., Stenbit,AE., Hatton,K., Depinho,R., and Charron,MJ. Cardiac and adipose tissue abnormalities but not diabetes in mice deficient in GLUT4. *Nature (London)* 1995, 377: 151-155
- [71]: Kopecky,J., Clarke,G., Enerback,S., Spiegelman,B., and Kozak,LP. Expression of the mitochondrial uncoupling protein gene from the aP2 gene promoter prevents genetic obesity. *J Clin Invest* 1995, 96: 2914-23
- [72]: Levak-Frank,S., Radner,H., Walsh,A., Stolberg,R., Knipping,G., Hoeflr,F., Sattler,W., Weinstoc,PH., Breslow,JL., and Zechner,R. Muscle-specific overexpression of lipoprotein-lapse causes a severe myopathy characterized by proliferation of mitochondria and peroxisomes in transgenic mice. *J Clin Invest* 1995, 96: 976-986
- [73]: Lowell, BB., Susulic,VS., Hamann,A., Lawitts,J., Boyer,B, Kozak, LP., and Flier,Js. Development of morbid obesity in transgenic mice following the genetic ablation of brown adipose tissue. *Clin Res* 1993, 41: 260A (abstr.)
- [74]: Richard,D., Chapdelaine,S., Deshaies,Y., Pepin,MC., and Barden,N. Energy balance and lipid metabolism in transgenic mice bearing an antisense GCR gene construct. *Am J Physiol* 1993, 265: R146-R150

- [75]: Shepherd,PR., Gnudi,L., Tozzo,E., Yang,HM., Leach,F., and Kahn,BB. Adipose cell hyperplasia and enhanced glucose disposal in transgenic mice overexpressing GLUT4 selectively in adipose-tissue. *J Biol Chem* 1993,268: 2243-46
- [76]: Stenzel-Poore, MP., Cameron,VA., Vaughan,J., Sawchenko,PE, and Vale, W. Development of Cushing's syndrome in corticotropin-releasing factor transgenic mice. *Endocrinology* 1992, 130: 3378-86
- [77]: Susulic,VS., Frederic, RC., Lawitts,J., Tozzo,E., Kahn,BB., Harpr,ME., Himmshagen,J., Flier,JS., and Lowell,BB. Targeted disruption of the beta 3 adrenergic receptor gene. *J Biol Chem* 1995, 270: 9483-92
- [78]: Gallo, RC. The AIDS virus. *Scient Am* 1987, 256: 46-56
- [79]: Fauci, AS. The human immunodeficiency virus: Infectivity and mechanisms of Pathogenesis. *Science* 1988, 239: 617-622
- [80]:Lusky, M., Botchan M. Inhibition of SV40 replication in simian cells by specific pBR32 DNA sequences. *Nature* 1981, 293: 79-81
- [81]: Schnieke, A., K. Harbers and R. Jaenisch. Embryonic lethal mutation in mice induced by retrovirus insertion into the  $\alpha 1(I)$  collagen gene. *Nature* 1983, 304: 316-320
- [82]: Woychick, RP., TA. Stewart, LG. Donis, P. D'Eustachio and P. Leder. An inherited limb deformity created by insertional mutagenesis in a transgenic mouse. *Nature* 1985, 318: 36-40
- [83]: Yokoyama, T., N.G. Copeland, N.A. Jenkins, C. A. Montgomery, F.F.B. Elder and P.A. Overbeek. Reversal of left-right asymmetry: a situs inversus mutation.

Science 1993, 260: 679-682

[84]: Triglia, T., Peterson MG. And David JK. A procedure for in vitro amplification of DNA segments that lie outside the boundaries of known sequences. *Nucleic Acids Research* 1986,16(16):8186

[85]: Yaoguang Liu and Robert FW. Thermal asymmetric interlaced PCR: automatable amplification and sequencing of insert end fragments from P1 and YAC clones for chromosome walking. *Genomics* 1995, 25: 674-681

[86]: Scherdin U., Rhodes K. and Breindl M. Transcriptionally active genome regions are preferred targets for retrovirus integration. *J Virol* 1990, 64(2): 907-912

[87]: Geoffey,MD., Suwon, K., Richard, MM., and David RC. Exon trapping: A genetic screen to identify candidate transcribed sequences in cloned mammalian genomic DNA. *Proc Natl Acad Sci USA* 1990, 87: 8995-99

[88]: Alan JB., David DC., Sharon LG., David JB., Daniel AH. Exon amplification: a strategy to isolate mammalian genes based on RNA splicing. *Proc Natl Acad Sci USA* 1991,88: 4005-9

[89]: George AB. Progress in understanding the genetics of obesity. *J Nutr* 1997, 127: 940S-942S

[90]: Beales,P.L., Kopelman, P.G. Obesity genes, *Clinic Endocrinology* 1996,45:373-78

[91]: Nadeau., J.H. Linkage and syntenic homologies between mouse and man. *The Jackson Laboratory*,12 March 1990.

[92]: Bouchard, C. The causes of obesity: advances in molecular biology but

- stagnation on the genetic front. *Diabetologia* 1996,39:1532-33
- [93]: Draznin,B., Sussman,K. The existence of an optimal range of cytosolic free calcium for insulin-stimulated glucose. *J.Biol.Chem.* 1987,262:15385-88
- [94]: Kelly,K.L.,Deeney,J.T. Cytosolic free calcium in adipocytes. Distinct mechanisms of regulation and effects on insulin action. *J.Biol.Chem.* 1989,264:12754-57
- [95]: Byyny,R.L., LoVerde,M. Cytosolic calcium and insulin resistance in elderly patients with essential hypertension. *Am, J. Hypertens.* 1992,5:459-64
- [96]: Zemel,M.B. Grunberger,G. Abstr *Am.J.Hypertens.* 1991,4:121
- [97]: Reusch,J.E.-B., Sussman,K.E. Inverse relationship between GLUT-4 phosphorylation and its intrinsic activity. *J.Biol.Chem.* 1993,268:3348-51
- [98]: Begum,N., Sussman,K.E. Calcium-induced inhibition of phosphoserine phosphatase in insulin target cells is mediated by the phosphorylation and activation of inhibitor 1. *J.Biol.Chem.* 1992,267:5959-63
- [99]: Begum,N., Sussman,K.E. High levels of cytosolic free calcium inhibit dephosphorylation of insulin receptor and glycogen synthase. *Cell Calcium*, 1991,12:423-30
- [100]: Guerro-Millo, M., Staels, B., Auwerx, J., New insights into obesity genes. *Diabetologia*, 1996,39:1528-31
- [101]: Bray,G.A., York, D.A. Hypothalamic and genetic obesity in experimental animals: an autonomic and endocrine hypothesis. *Physiol. Rev.* 1979,59:719-809

- [102]: Noben-Trauth, K., Naggert, J.K. A candidate gene for the mouse mutation tubby. *Nature* 1996,380:534-38
- [103]: Kley, P.W., Wei Fan, Steve G., Kovats, John J.Lee. et al. Identification and characterization of the mouse obesity gene tubby: a member of a novel gene family. *Cell* 1996,85: 281-290
- [104]: Zauli, G., Gibellini, D. The human immunodeficiency virus type-1 (HIV-1) tat protein and Bcl-2 gene expression. *Leukemia and Lymphoma* 1996,23:551-60
- [105]: Barbanit-Brodano, G., Sampaolesi, R. HIV-1 tat acts as a growth factor and induces angiogenic activity in BK virus/tat transgenic mice. *Advanced Technologies in Research, Diagnosis and treatment of AIDS and in Oncology. Antibiot Chemother. Basel, Karger*, 1994,46:88-101
- [108]: Vogel, J., Hinrichs, S.H., Kay Reynolds, R., Luciw, P.A. and Jay, G. The HIV tat gene induces dermal lesions resembling kaposi's sarcoma in transgenic mice. *Nature* 1988,335:606-611
- [107]: Li, S.W., Nembhard, K.M. Identification and cloning of integration site of DNA by PCR. *Bio Techniques* 1996,20:356-58
- [108]: Stubbs, L. Long-range walking techniques in positional cloning strategies. *Mammalian Genome*. 1992,3:127-42

## **Appendix I**

### **A) Media Used**

#### **i) TB Medium and Plates**

in 950 ml ddH<sub>2</sub>O add:

10 grams NaCl

20 grams Yeast Extract

20 grams Bacto Tryptone

Adjust pH to 7.0 with 5M NaOH, bring up volume to

1 litre and autoclave.

If necessary add 100 mg Ampicillin (100ug/ml)

For TB Plates 15 g/l of Agar is added.

#### **ii) SOC Medium**

in 950 ml ddH<sub>2</sub>O add:

0.5 grams NaCl

5 grams Yeast Extract

20 grams Bacto Tryptone

10 ml of 0.2 M KCl

Adjust pH to 7.0 with 5M NaOH, bring up volume to

1 litre and autoclave.

Add 5 ml of sterile 2M MgCl<sub>2</sub>

Add 10 ml of sterile 2M Glucose

## **B) Solutions Used**

i) TE buffer (10mM Tris ,1 mM EDTA)

to 988 ml ddH<sub>2</sub>O add:

10 ml of 1 M Tris.Cl (pH 8.0)

2 ml of 0.5 M EDTA (pH 8.0)

ii) 5 x TBE

in 1 litre ddH<sub>2</sub>O add:

54 grams of Tris base

27.5 grams of boric acid

20 ml of 0.5 M EDTA (pH 8.0)

mix well and autoclave.

ii) Buffers for Alkaline Lysis Preparation of plasmid

Solution I: 50 mM glucose

25 mM Tris.Cl (pH 8.0)

10 mM EDTA (pH 8.0)

Autoclave and store at 4°C.

Solution II: 0.2 N NaOH (freshly diluted from a 10 N stock)

1% SDS

Solution III: 5 M potassium acetate    60 ml

Glacial acetic acid            11.5 ml



in 800 ml ddH<sub>2</sub>O add:

175.3 g NaCl

27.6 g NaH<sub>2</sub>PO<sub>4</sub>·H<sub>2</sub>O

7.4 g EDTA

Adjust the pH to 7.4 with 10 N NaOH and adjust the volume to

1 litre with ddH<sub>2</sub>O. Autoclave.

vii) Prehybridization solution

3	ml	20x SSPE
1	ml	50x Denhardt's
0.1	ml	Salmon Sperm DNA(10mg/ml)
0.125	ml	2 M Sodium phosphate(pH6.5)
5	ml	Formamide
0.775	ml	ddH <sub>2</sub> O

Hybridization solution

3	ml	20x SSPE
1	ml	50x Denhardt's
0.1	ml	Salmon Sperm DNA(10mg/ml)
0.125	ml	2 M Sodium phosphate (pH6.5)
5	ml	10% Dextran sulfate (in formamide)
0.8	ml	ddH <sub>2</sub> O

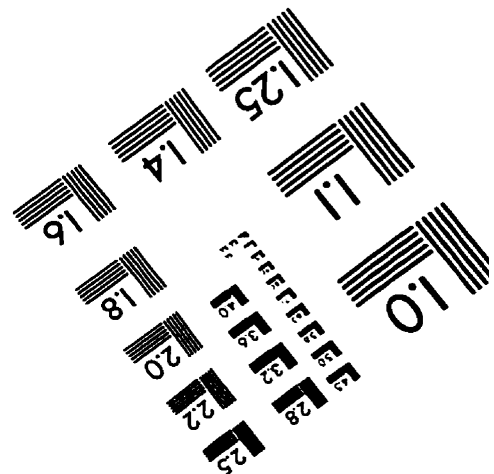
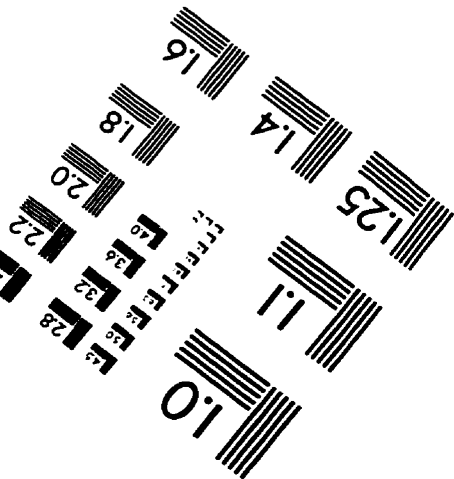
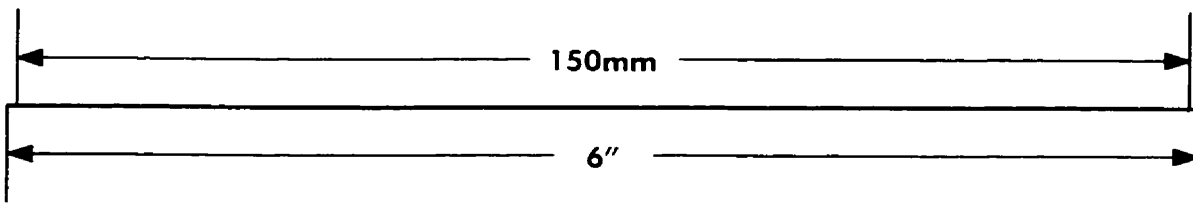
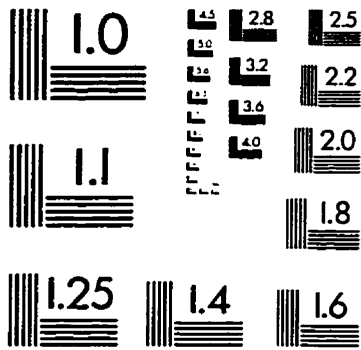
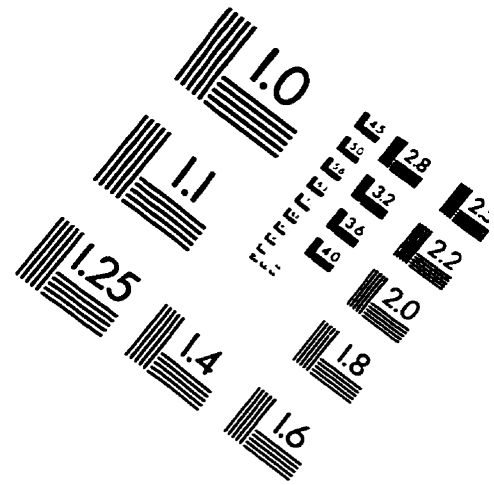
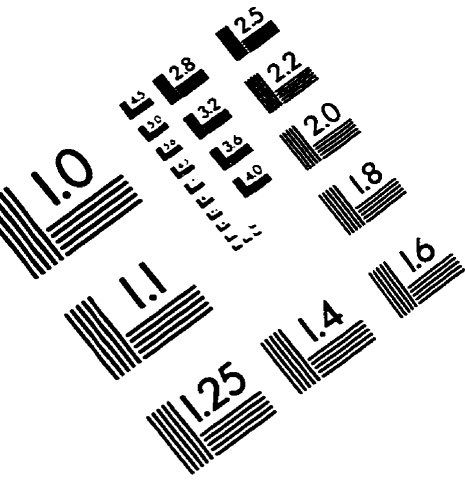
viii) 1 x PCR buffer

10	mM	Tris.Cl (pH9.0 )
----	----	------------------

1.5 mM MgCl<sub>2</sub>

50 mM KCl

# IMAGE EVALUATION TEST TARGET (QA-3)



**APPLIED IMAGE, Inc**  
 1653 East Main Street  
 Rochester, NY 14609 USA  
 Phone: 716/482-0300  
 Fax: 716/288-5989

© 1993, Applied Image, Inc., All Rights Reserved